Diplomarbeit

REGULATION OF TUMOR CELL MIGRATION IN NON-SMALL CELL LUNG CANCER

eingereicht von

Martin Zacharias

zur Erlangung des akademischen Grades

Doktor der gesamten Heilkunde
(Dr. med. univ.)

an der
Medizinischen Universität Graz

ausgeführt an der / am

Universitätsklinik für Innere Medizin / Institut für Pathologie

unter der Anleitung von

Assoz. Prof. Mag. Dr. Nadia Dandachi

DDr. Luka Brcic

Graz, 29.10.2017

Eidesstattliche Erklärung

Ich erkläre ehrenwörtlich, dass ich die vorliegende Arbeit selbstständig und ohne fremde Hilfe verfasst habe, andere als die angegebenen Quellen nicht verwendet habe und die den benutzten Quellen wörtlich oder inhaltlich entnommenen Stellen als solche kenntlich gemacht habe.

Graz, am 29.10.2017 Martin Zacharias eh

DECLARATION

The following thesis is based on a manuscript, which we have submitted for publication in a peer-reviewed journal:

Popper HH, Eidenhammer S, Zacharias M, Brcic L. Bulk tumor cell migration in lung carcinomas is more common than epithelial-mesenchymal transition and differently regulated. Manuscript submitted for publication
Corresponding Author: Univ. Prof. Dr. Helmut H. Popper, Head of the Research Unit for Molecular Lung & Pleura Pathology, Institute of Pathology, Medical University of Graz, Austria

First results of this study were presented as a poster at the AACR Annual Meeting 2017:

Popper HH, Eidenhammer S. Bulk lung cancer cell migration is more common than single cell migration and regulated by different genes [abstract]. In: Proceedings of the American Association for Cancer Research Annual Meeting 2017; 2017 Apr 1-5; Washington, DC. Philadelphia (PA): AACR; Cancer Res 2017;77(13 Suppl): Abstract nr 1880. doi:10.1158/1538-7445.AM2017-1880

ACKNOWLEDGEMENTS

First, I would like to thank DDr. Luka Brcic for his supervision and for his great efforts to support me in every aspect of this thesis. Being his student and working with him was really a pleasure.

Furthermore, I want to thank Prof. Dr. Nadia Dandachi for her supervision and for her excellent suggestions, which helped to improve the quality of this thesis.

Special thanks go to Prof. Dr. Helmut H. Popper for giving me the opportunity to be part of this study and for fruitful discussions about this fascinating topic.

Last but not least, I would like to thank my family for supporting me in every possible way throughout my studies.

ABSTRACT

Due to the nonmotile nature of adult epithelia, carcinomas are considered to undergo an epithelial-to-mesenchymal transition (EMT) before they start to migrate. However, histopathological findings provide evidence for an alternative mode of tumor cell migration beyond classical EMT: Instead of migrating as separated single cells, which would be the logical consequence of a complete EMT-program, carcinomas often move in multicellular complexes. Despite these facts, relatively little is known about the actual mechanisms behind the movement of tumor cell bulks.

Therefore, we aimed to further examine bulk cell migration in non-small cell lung cancer (NSCLC) patient samples using immunohistochemistry.

As a first step, 30 surgically resected NSCLC specimens were immunohistochemically evaluated in terms of expression and distribution of EMT-markers and molecules associated with migration and metastasis in general. The selected cases were all characterized by vascular invasion. Consequently, the expression of the respective markers was compared between the primary tumor, the invasion front, and the vascular invasion site. Finally, to validate our findings in a larger cohort and to avoid a selection bias, tissue microarrays with 528 NSCLC cases were additionally evaluated for selected markers of interest.

Twist was the only EMT transcription factor which was expressed in all cases of the study set. However, TGFß, a molecule known to upregulate Twist and induce EMT, was negative in all cases. Snail was only minimally expressed in less than half of our cases. The fact that ZEB1 and Slug were both negative in almost all tumors, provides further evidence for an incomplete EMT. The coexpression of E-cadherin and N-cadherin in all 30 cases of the study set indicates a cell phenotype that is not exclusively mesenchymal or epithelial, but rather a state in between. The markers pERK, RhoA, FAK, ILK, and YAP1 were downregulated at the invasive sites compared to the tumor center. Conversely, the markers Vimentin, Mad, Brk, Rab40B, Tks5, Fascin, and PLCγ were clearly upregulated at the invasive sites.

In conclusion, presented data provide evidence of significant differences in the expression of involved molecules between single cell and collective cell invasion, including the presence of a partial EMT rather than EMT in its classical binary form.

ZUSAMMENFASSUNG

Da adultes Epithelgewebe als migrationsunfähig gilt, wird angenommen, dass Karzinome vor der Invasion eine epithelial-mesenchymale Transition (EMT) durchlaufen. Histopathologische Beobachtungen führen allerdings zur Frage nach alternativen Erklärungsmodellen abseits der klassischen EMT: Anstelle einer Migration von getrennten Einzelzellen, was die logische Konsequenz eines kompletten EMT-Programms wäre, migrieren Karzinome nämlich oft als multizelluläre Komplexe. Trotz dieser Befunde ist über die Mechanismen, die hinter einer Migration von Tumorzellkomplexen stehen, nur wenig bekannt.

Das Ziel unserer Studie war es deshalb, die Migration von Tumorzellkomplexen in Patientenproben nicht-kleinzelliger Lungenkarzinome (NSCLC) mittels Immunhistochemie genauer zu charakterisieren.

Zuerst wurden 30 operativ entfernte NSCLC-Proben in Hinblick auf die Expression und Verteilung von EMT-Markern und anderen Migrations- und Metastasierungs-assoziierten Molekülen immunhistochemisch untersucht. Dabei waren alle 30 Fälle durch eine vaskuläre Invasion gekennzeichnet. Folglich wurde die Expression der jeweiligen Marker zwischen Primärtumor, Invasionsfront und vaskulärem Invasionsgebiet verglichen. Um unsere Ergebnisse in einer größeren Kohorte zu validieren und einen Selektionsbias zu verhindern, wurden bei 528 Fällen zusätzlich Tissue-Microarrays angefertigt und auf die Expression ausgewählter Marker untersucht.

Twist war der einzige EMT-Transkriptionsfaktor, der in allen Fällen des Study-Sets exprimiert war. TGFß, ein Molekül mit der Eigenschaft Twist hochzuregulieren und eine EMT zu induzieren, war jedoch in allen Fällen negativ. Snail war in weniger als der Hälfte der Fälle, und hier nur geringfügig, exprimiert. Die Negativität von ZEB1 und Slug in fast allen Tumoren kann als weiterer Hinweis einer nur inkompletten EMT gewertet werden. Die Koexpression von E-Cadherin und N-Cadherin in allen Fällen des Study-Sets verweist auf einen nicht ausschließlich mesenchymalen oder epithelialen Zell-Phänotyp, sondern vielmehr auf einen Zustand zwischen diesen beiden Polen. Die Marker pERK, RhoA, FAK, ILK und YAP1 waren, im Vergleich zum Tumorzentrum, in den Invasionsgebieten

herunterreguliert. Dagegen waren die Marker Vimentin, Mad, Brk, Rab40B, Tks5, Fascin und PLCγ in den Invasionsgebieten hochreguliert.

Zusammengefasst liefern die vorliegenden Daten Hinweise darauf, dass es zwischen der Einzelzellinvasion und der kollektiven Zellinvasion erhebliche Unterschiede in der Expression beteiligter Moleküle gibt. Insbesondere scheint eher eine partielle EMT als die klassische binäre EMT vorzuliegen.

TABLE OF CONTENTS

LIST OF ABBREVIATIONS

AC	adenocarcinoma
AEC	aminoethyl carbazole
ALK	anaplastic lymphoma kinase
AP-1	activator protein 1
ATF	activating transcription factor
BATF2	basic leucine zipper ATF-like transcription factor 2
BMP7	bone morphogenic protein 7
Brk	brinker
CC1	cell conditioning solution 1
CCL2	C-C motif chemokine ligand 2
CD56	cluster of differentiation 56; also known as NCAM
CdC42	cell division control protein 42 homolog
CDKN2A	cyclin-dependent kinase inhibitor 2A
CK5	cytokeratin 5
Con43	connexin 43
CSC	cancer stem cell
CT	computed tomography
CTC	circulating tumor cell
CXCR	C-X-C motif chemokine receptor
DAB	3,3'-diaminobenzidine
DNA	deoxyribonucleic acid
DR6	death receptor 6
DUTT1	deleted in U twenty twenty; also known as ROBO1
EBUS	endobronchial ultrasound
E-Cad	E-cadherin
EGFR	epidermal growth factor receptor
EMT	epithelial-to-mesenchymal transition
EPHA7	ephrin type-A receptor 7
ERK	extracellular-signal regulated kinase
FAK	focal adhesion kinase
FFPE	formalin-fixed, paraffin-embedded

FHIT	fragile histidine triad
FUS1	fusion 1 protein; also known as TUSC2
G-CSF	granulocyte-colony stimulating factor
GDP	guanosine diphosphate
G-Protein	guanine nucleotide-binding protein
GTP	guanosine triphosphate
HER2	human epidermal growth factor receptor 2
HIV	human immunodeficiency virus
HRP	horseradish peroxidase
IFN	interferon
IHC	immunohistochemistry
ILK	integrin-linked kinase
KRAS	Kirsten rat sarcoma oncogene
LC	large cell carcinoma
LCNEC	large cell neuroendocrine carcinoma
Mad	mothers against decapentaplegic
MAD1L1	mitotic arrest deficient 1-like protein 1
MAPK	mitogen-activated protein kinase
MET	mesenchymal-to-epithelial transition
MLL	mixed-lineage leukemia protein
MRI	magnetic resonance imaging
MW	microwave
N-Cad	N-cadherin
NCAM	neural cell adhesion molecule; also known as CD56
NET	neutrophil extracellular traps
NGS	next-generation sequencing
NK-cell	natural killer cell
NRG1	neuregulin 1
NSCLC	non-small cell lung cancer
NTRK1	neurotrophic receptor tyrosine kinase 1
PD-(L)1	programmed death (ligand) 1
pERK	phosphorylated extracellular-signal regulated kinase
PET	positron emission tomography
PLCγ	phospholipase C gamma

PTEN	phosphatase and tensin homolog
Rack1	receptor for activated C kinase 1
RASSF1	ras association domain family member 1
RB1	retinoblastoma 1
RhoA	ras homolog gene family member A
ROBO1	roundabout guidance receptor 1; also known as DUTT1
SARI	suppressor of AP-1, regulated by IFN
Sax	saxophone
SCC	squamous cell carcinoma
SCLC	small cell lung cancer
SMARCA4	SWI/SNF related, matrix associated, actin dependent regulator of chromatin, subfamily A, member 4
SPN	solitary pulmonary nodule
SWI/SNF	switch/sucrose nonfermentable
TGFß	transforming growth factor beta
TKI	tyrosine kinase inhibitor
Tks5	tyrosine kinase substrate 5
TMA	tissue microarray
TNM	Tumor-Node-Metastasis
TP53	tumor protein p53
TPC	tunneled pleural catheter
TPS	tumor proportion score
TTF-1	thyroid transcription factor 1
TUSC2	tumor suppressor candidate 2; also known as FUS1
UV	ultraView
VATS	video assisted thoracoscopy
VEGF(R)	vascular endothelial growth factor (receptor)
VHL	Von Hippel-Lindau tumor suppressor
Vim	vimentin
WHO	world health organization
Wnt	wingless-related integration site
YAP	yes-associated protein
ZEB1	zinc finger E-box binding homeobox 1
ZFPL1	zinc finger protein-like 1

LIST OF FIGURES

LIST OF TABLES

1 INTRODUCTION

1.1 Lung cancer

1.1.1 Epidemiology

Worldwide, lung cancer is the leading cause of cancer-related death in both men and women. In 2012, approximately 1.8 million people were diagnosed with lung cancer, and about 1.6 million patients died of lung cancer. Because of an increase in global tobacco use it is estimated that deaths due to lung cancer will continue to rise. While in most industrialized countries the incidence of lung cancer is declining, in many developing countries the incidence is rising. These trends are clearly associated with changes in smoking habits. The global distribution of lung cancer incidence and mortality is summarized in Figure 1:

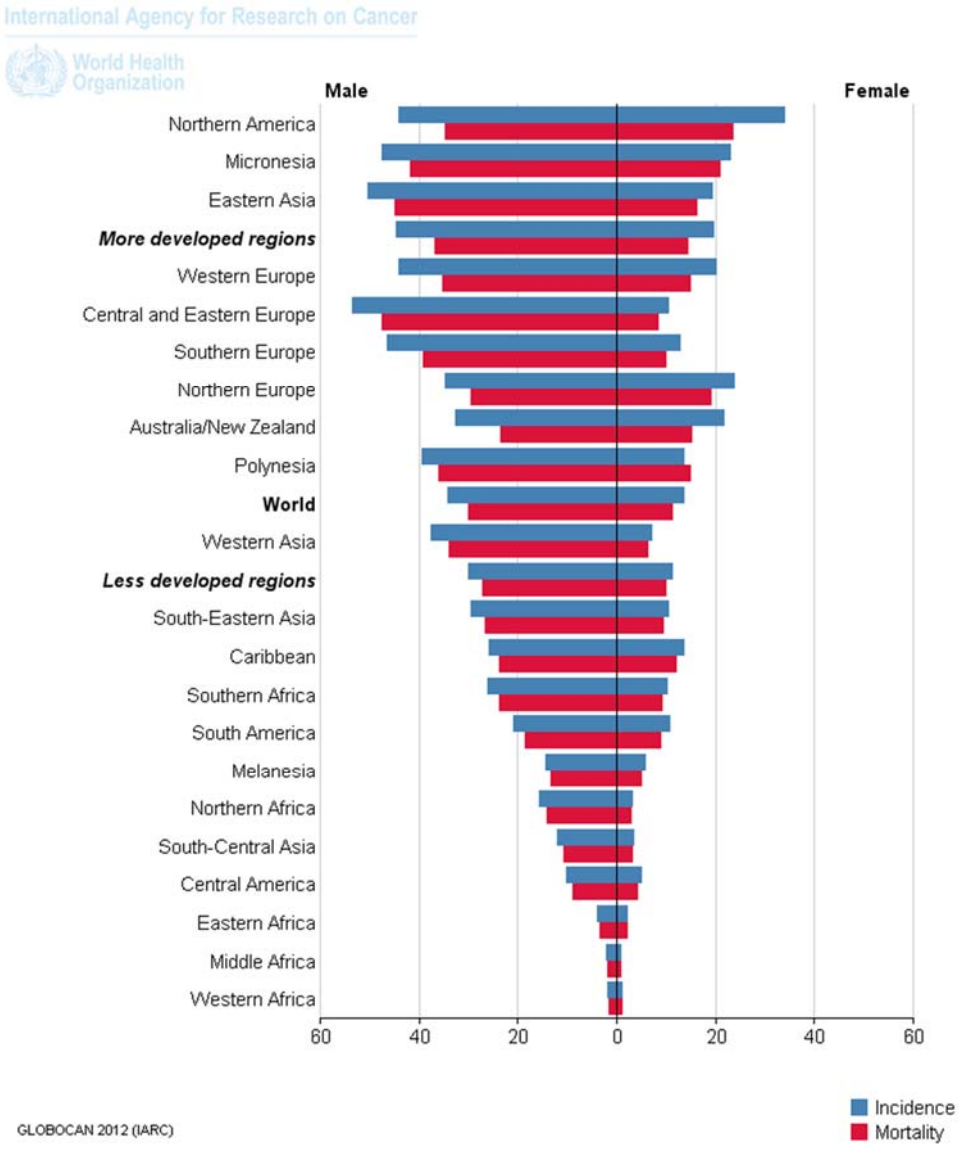

Figure 1: Worldwide lung cancer rates in 2012 (per 100,000). From: GLOBOCAN 2012 (1)

The highest incidence rates in men are observed in Central and Eastern Europe (53.5 per 100,000) and the lowest are seen in Western Africa (1.7 per 100,000). In women, the incidence rates are generally lower compared to those in men and are highest in Northern America (23.7 per 100,000) and lowest in Middle Africa (0.8 per 100,000). (1–3)

In Europe, lung cancer is the leading cause of cancer death in men, but not in women. However, for women between the ages of 45 and 74 years, more deaths from lung than breast cancer were predicted for 2017. Breast cancer is the primary cause of cancer-related death only in young and elderly women. For men, lung cancer mortality declines since the 1980s, while for women it continues to rise. Only in the younger age group (between the ages of 25 and 44 years), rates are predicted to be similar for women and men, reflecting disparities in gender-specific smoking habits across different generations. These predictions and trends confirm that smoking has the same impact on lung cancer in both men and women (4). According to a study from 2013 (5), there are remarkable differences in the lung cancer incidence rate between different European countries, ranging from 49 cases/100 000 in Cyprus to 156 cases/100 000 in Hungary. For women, the highest incidence rate is seen in Northern Europe and the lowest in Eastern European countries, whereas for men the lowest is seen in Northern European countries and the highest in Central and Eastern Europe (5).

In Austria, lung cancer is, after prostate cancer, the second most common type of cancer in men (2.894 newly diagnosed in 2014), and, after breast and colon cancer, the third most common in women (1.822 newly diagnosed in 2014). In men, lung cancer is the most common cause of cancer death (2.450 died in 2014), while in women it is, after breast cancer, the second most common cause of cancer death (1.450 died in 2014). Consistent with worldwide and European trends in the last decade, both incidence and mortality rates increased in women (21% and 22%, respectively) and decreased in men (13% and 14%, respectively). Geographically, Vienna showed both the highest incidence and mortality rates within Austria, whereas the lowest incidence rate was seen in Upper Austria and the lowest mortality rate in Salzburg. In general, the survival rates increased over time (both 1- and 5-year survival) and showed some differences between women and men (5-year survival rate 23% and 16% respectively). (6)

Risk factors for the development of lung cancer comprise tobacco (including secondhand smoke), radon, asbestos, and many other environmental factors. However, as smoking is attributable to 80-85% of lung cancer deaths, it is by far the most important one. Compared to never-smokers, the incidence rate is approximately 20 times increased in people who smoke one pack of cigarettes per day for 40 years (7,8). Still, the risk of individuals who quit smoking falls significantly, especially in those who quit in younger age (9). Consequently, smoking cessation and, more importantly, preventing people from starting to smoke are the most important aspects of reducing the incidence and mortality of lung cancer.

In addition to the aforementioned inhalation toxins, other factors increasing the risk of lung cancer comprise: pulmonary fibrosis (7-fold increased risk (10)), radiation therapy, HIV infection, genetic factors, and probably dietary factors and alcohol (11). In the etiology of lung cancer both exposure to risk factors and individual susceptibility to those factors are important. Furthermore, the lung cancer risk can be augmented by synergistic interactions among different agents. A well-described example of this interaction is the synergistic effect of cigarette smoking with asbestos exposure and radon (12).

1.1.2 Classification and morphological aspects

The classification of lung cancer should be done according to the 2015 World Health Organization (WHO) classification of lung tumors (13,14). For a long time, the only clinical relevant information was the differentiation between small cell lung cancer (SCLC) and non-small cell lung cancer (NSCLC). Since the precise classification of histological subtypes has now ever increasing prognostic and predictive significance, they will be discussed in more detail (13,15,16).

Adenocarcinomas comprise about 50% of all lung cancer cases, and are therefore the most common histological type in the western world (14). For decades, an increased incidence has been observed in pulmonary adenocarcinomas. One possible explanation for that, although still controversial, is the consumption of low-tar filter cigarettes, which have been introduced in the mid-20th century (14,17). Histologically, lung adenocarcinomas are characterized by neoplastic gland formation, the appearance of intracytoplasmic mucin, and/or by pneumocyte marker expression (TTF-1, napsin A) (14). In the WHO classification, it is specified that one of these three characteristics is sufficient to establish the diagnosis of lung adenocarcinoma (13,14). The genetic profile of adenocarcinoma comprises several driver gene alterations, including EGFR, KRAS, BRAF, ERBB2/HER2, ALK, ROS1, RET, NTRK1, and NRG1. Because approved targeted drugs are available for patients whose tumors harbor mutations in EGFR, ALK or ROS1, these are the most clinically relevant ones (13,14). The morphology of neoplastic structures can vary significantly in different adenocarcinomas, leading to further subtyping of growth patterns (acinar, papillary, micropapillary, lepidic, and solid) with additional variants (mucinous, cribriform, colloid, fetal, and enteric) (13,14). The presence of these different patterns has prognostic significance (13,14,18,19). In the following, different cases of adenocarcinoma with typical growth patterns and variants are shown (Figures 2-9).

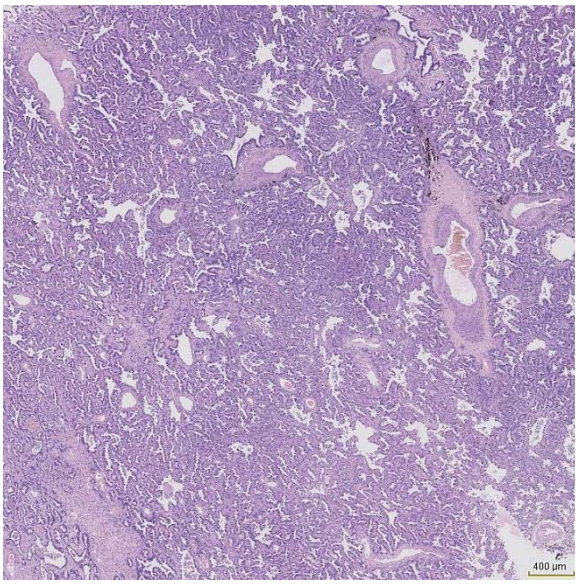

Figure 2: Low power view of an acinar adenocarcinoma; HE-staining; Scale bar 400 µm

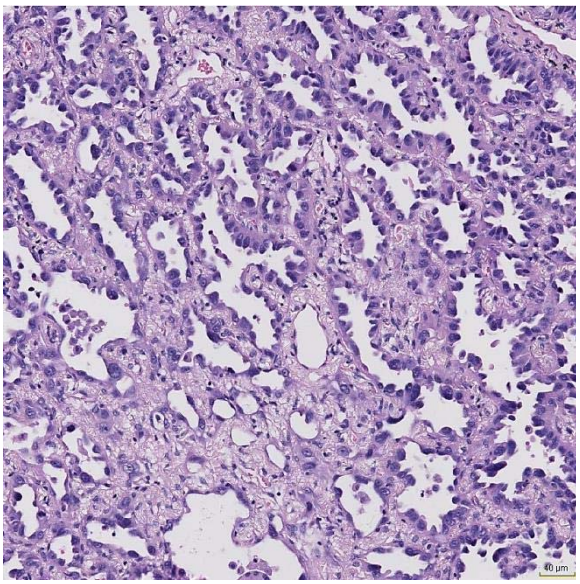

Figure 3: High power view of an acinar adenocarcinoma; HE-staining; Scale bar 40 µm

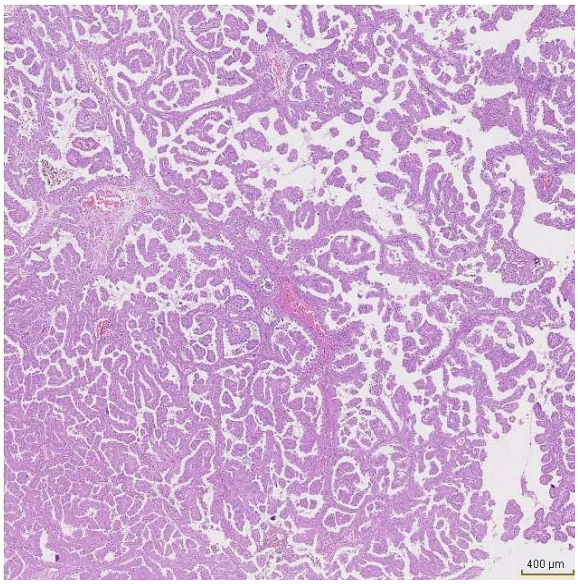

Figure 4: Low power view of a papillary adenocarcinoma; HE-staining; Scale bar 400 µm

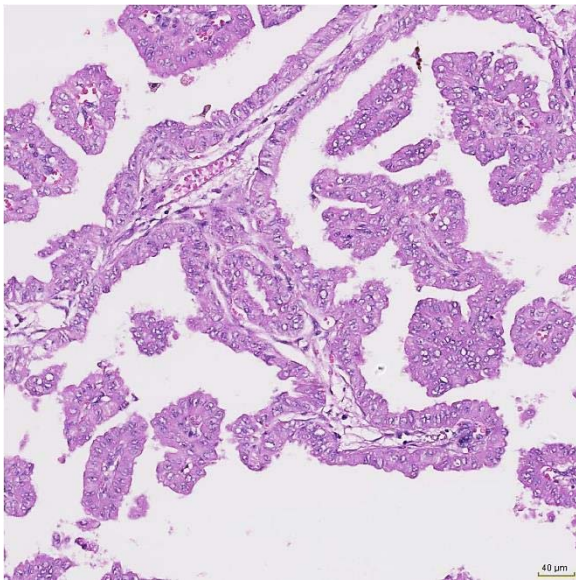

Figure 5: High power view of a papillary adenocarcinoma; HE-staining; Scale bar 40 µm

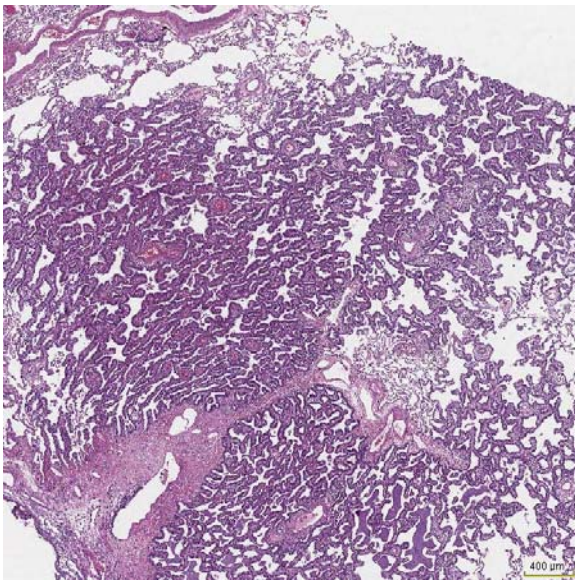

Figure 6: Low power view of a lepidic adenocarcinoma; HE-staining; Scale bar 400 µm

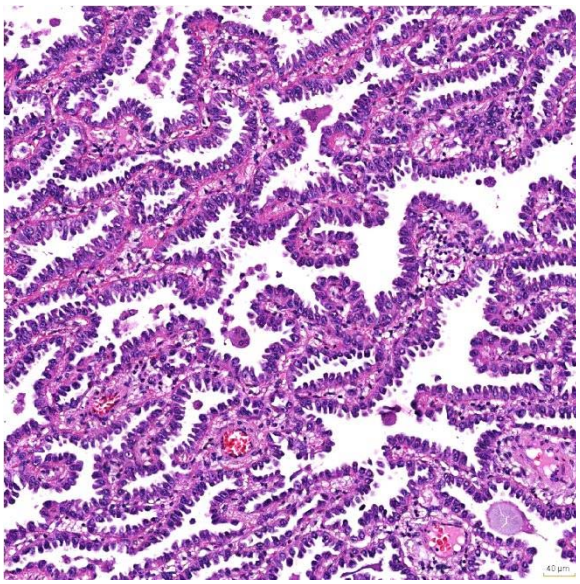

Figure 7: High power view of a lepidic adenocarcinoma; HE-staining; Scale bar 40 µm

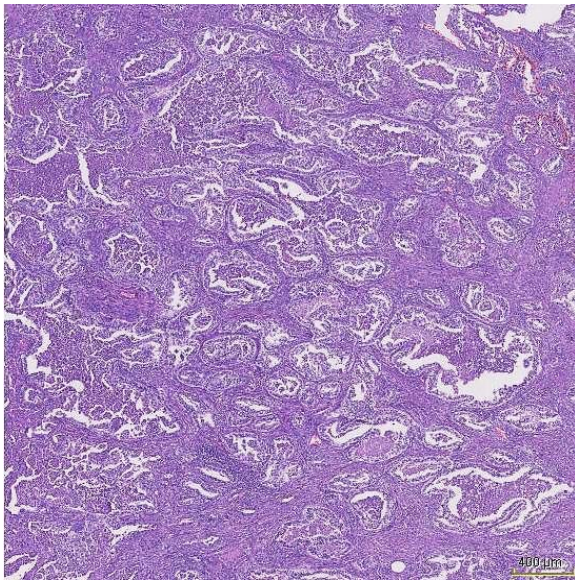

Figure 8: Low power view of a fetal variant of adenocarcinoma; HE-staining; Scale bar 400 µm

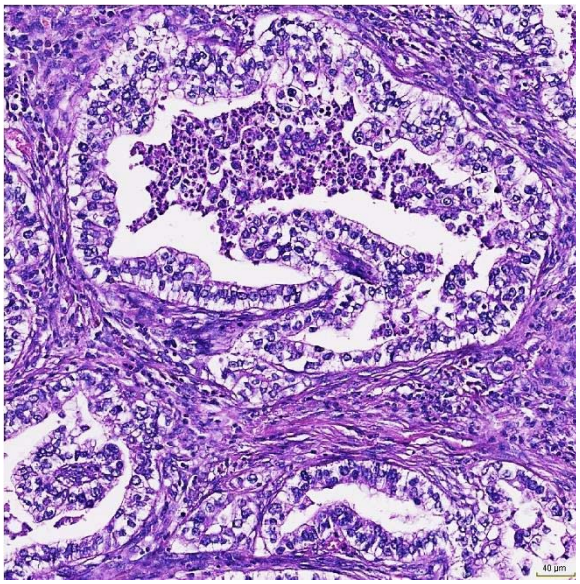

Figure 9: High power view of a fetal variant of adenocarcinoma; HE-staining; Scale bar 40 µm

Squamous cell carcinomas (Figures 10-12) are, after adenocarcinomas, the second most common histological type of lung cancer and arise mostly in the proximal tracheobronchial tree (13,14). They are characterized by intercellular desmosomes (Figure 11), keratin production by tumor cells (Figure 12), and/or the expression of specific markers, e.g. p40, p63, CK5 (13,14). Squamous cell carcinomas are divided into the following subtypes: non-keratinizing (no keratinization at all), keratinizing (at least some keratinization), and basaloid

(more than 50% of the tumor has basaloid features) (13,14). Since some adenocarcinomas show a squamous-like morphology (20), it is recommended to use immunohistochemistry to distinguish between non-keratinizing squamous cell carcinomas, solid type adenocarcinomas, and large cell carcinomas (13,14).

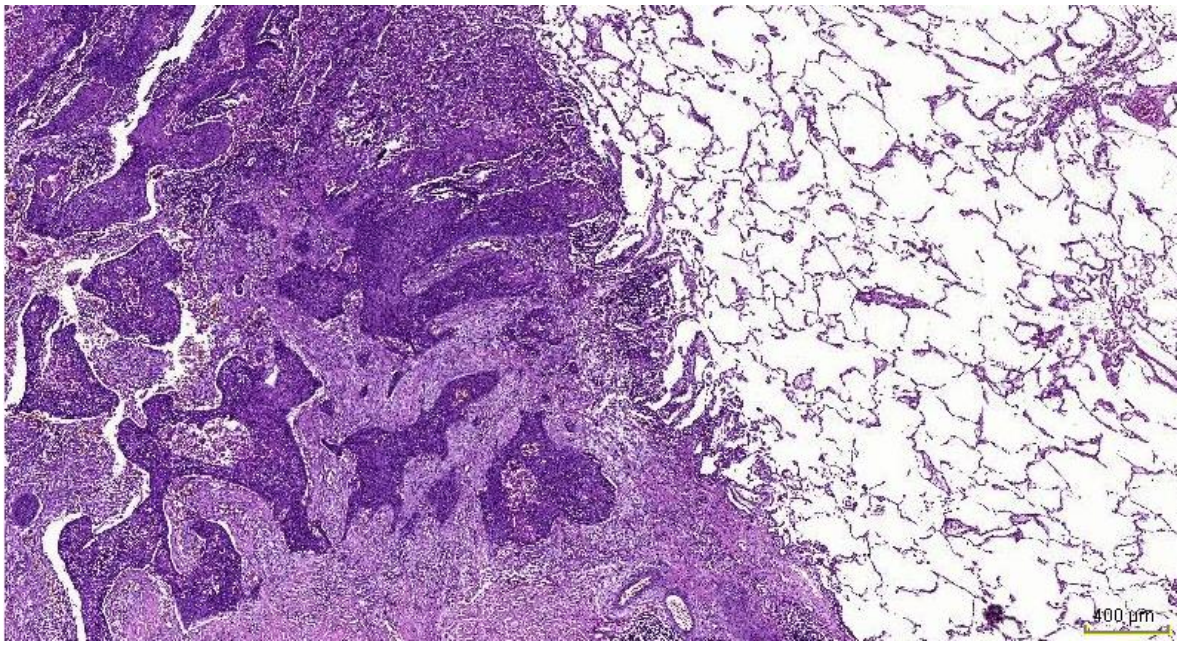

Figure 10: Low power view of a squamous cell carcinoma (on the left) and normal lung tissue (on the right); HE-staining; Scale bar 400 µm

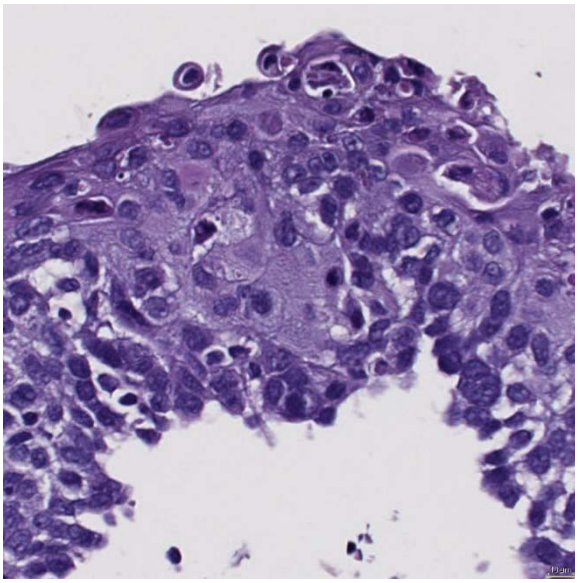

Figure 11: Intercellular bridges (desmosomes) within a squamous cell carcinoma; HE-staining; Scale bar 10 µm

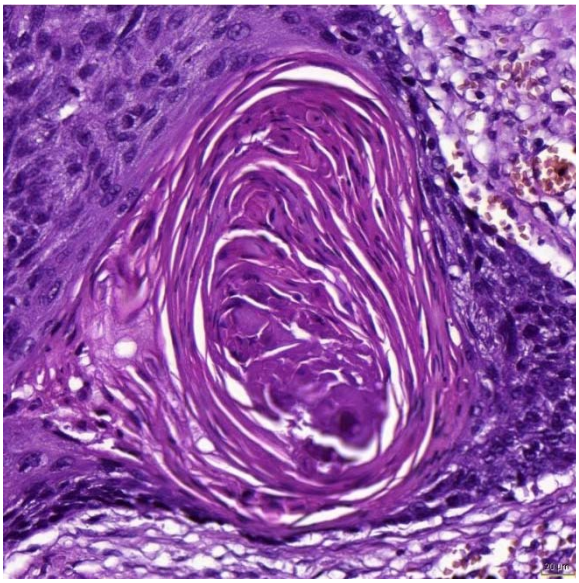

Figure 12: Keratinization within a squamous cell carcinoma; HE-staining; Scale bar 20 µm

Adenosquamous carcinomas are composed of both glandular and squamous components (at least 10% each) and account for 0.4 to 4 percent of pulmonary carcinomas (14). They are extremely aggressive and have a poorer prognosis than adenocarcinomas and squamous cell carcinomas (13,14,21). Because of the glandular component it is recommended to perform molecular testing for abnormalities in EGFR and ALK (13,14).

Large cell carcinoma is a poorly differentiated NSCLC and is a diagnosis of exclusion. It lacks both squamous and glandular differentiation (examined via light microscopy and immunohistochemistry), and also the cytological features of small cell carcinoma are missing (13,14). Typically, the tumor cells have vesicular nuclei, prominent nucleoli, and abundant eosinophilic cytoplasm (Figure 13 and Figure 14). Because of the so-called null phenotype of large cell carcinomas, it is not appropriate to apply that term to cytology specimens and small endoscopic biopsies. In these cases, the term “non-small cell lung cancer, not otherwise specified” is recommended (13,14). The incidence of large cell carcinomas has apparently decreased, since several entities, formerly classified as large cell carcinoma, were reclassified with the help of immunohistochemistry (e.g. TTF-1 expression for adenocarcinoma, p40 expression for squamous cell carcinoma, chromogranin and synaptophysin expression for neuroendocrine carcinoma) (13,14).

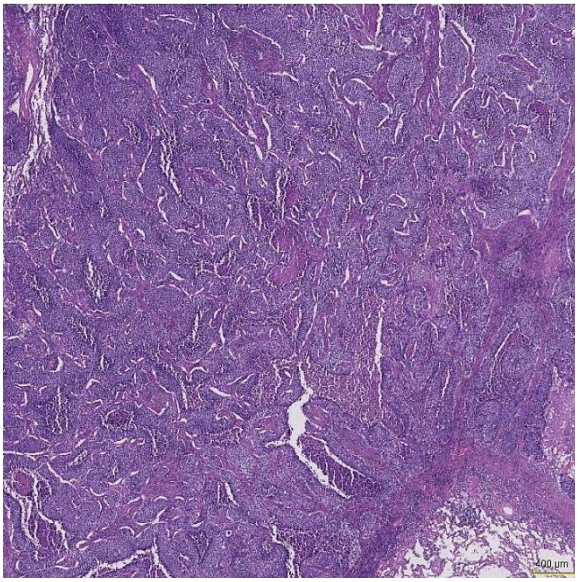

Figure 13: Low power view of a large cell carcinoma; HE-staining; Scale bar 400 µm

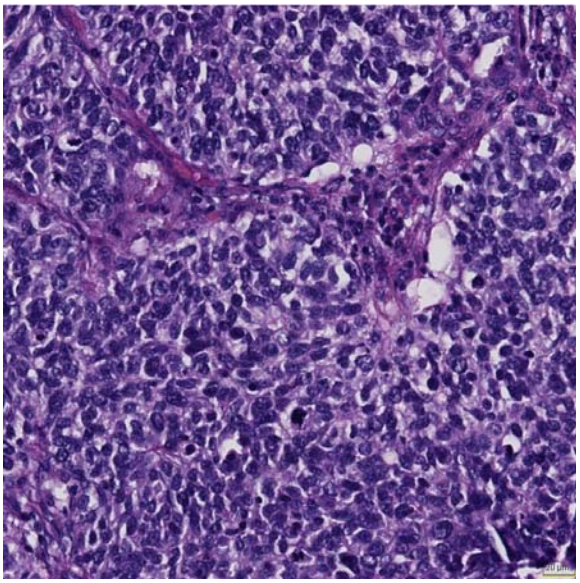

Figure 14: High power view of a large cell carcinoma; HE-staining; Scale bar 20 µm

Pleomorphic, spindle cell, and giant cell carcinomas together comprise less than 1% of all lung cancers and are associated with a poor prognosis (22). Pleomorphic carcinoma is a NSCLC with poor differentiation that contains spindle and/or giant cells (at least 10%). Spindle cell carcinoma consists almost entirely of epithelial spindle cells, whereas giant cell carcinoma consists of an almost pure population of tumor giant cells. Both spindle cell and giant cell carcinoma have no differentiated carcinomatous elements (13,14).

Neuroendocrine tumors include several tumor types which share neuroendocrine features. These subtypes are small cell lung carcinoma (SCLC), large cell neuroendocrine carcinoma (LCNEC), typical carcinoid, and atypical carcinoid. In general, SCLC and LCNEC have more necrosis and a much higher mitotic rate compared to pulmonary carcinoids (13,14,23).

Small cell lung carcinomas (SCLC) comprise around 13% of all pulmonary carcinomas, and are in almost all cases associated with smoking, hence extremely rare in persons who have never smoked (13,14). Histologically, they consist of cells with scant cytoplasm, poorly defined cell borders, absent or unobtrusive nucleoli, and finely dispersed granular nuclear chromatin. The cells are round, oval, or spindle-shaped, and the size of cells can be compared to the size of three resting lymphocyte nuclei. Typically, the mitotic count is high and necrosis is extensive (Figure 15 and Figure 16). In most cases small cell carcinomas express neuroendocrine markers like CD56, chromogranin or synaptophysin (13,14). There are several molecular abnormalities associated with SCLC, including amplification of the MYC and MAD1L1 gene, as well as extensive and multiple site deletions in chromosome 3p. These 3p sites contain many tumor suppressor genes: FHIT, RASSF1, FUS1, VHL, and DUTT1, among others. SCLC has a very poor prognosis, with a 2-year survival rate of only 10%. (13)

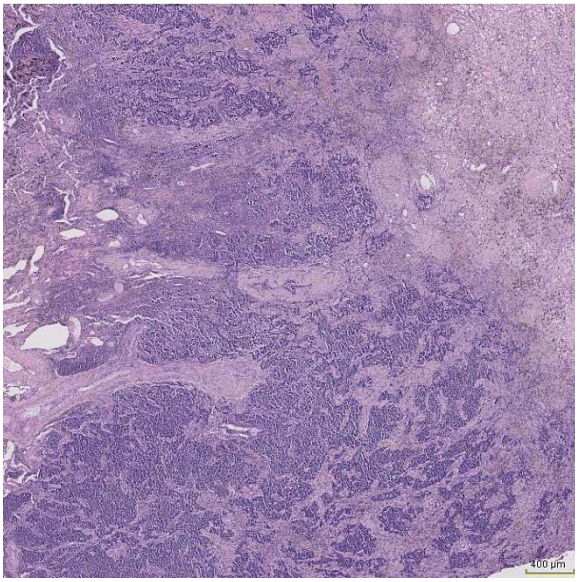

Figure 15: Low power view of a small-cell lung carcinoma with widespread necrotic areas; HE-staining; Scale bar 400 µm

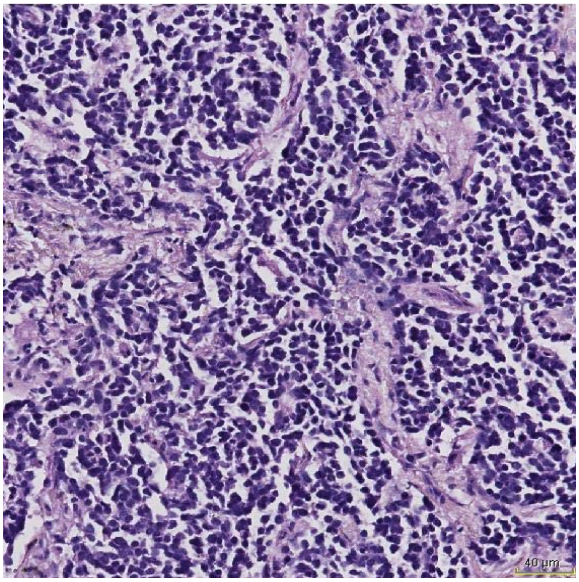

Figure 16: High power view of a small-cell lung carcinoma consisting of typical tumor cells with scant cytoplasm; HE-staining; Scale bar 40 µm

Large cell neuroendocrine carcinoma (LCNEC) is defined as a NSCLC that expresses at least one neuroendocrine marker and shows histological features of neuroendocrine morphology. As it is strongly related to smoking, more than 90% of these tumors occur in heavy smokers. In general, LCNEC is considered to be a high-grade tumor. Mostly it is located in the peripheral lung, although in 20% of cases a central location occurs (13,14). Histologically, LCNEC shows rosette-like structures, peripheral palisading, organoid nesting, and trabecular growth. The tumor cells have moderate to abundant cytoplasm and are generally large with often prominent nucleoli. LCNEC exhibits a very high mutation rate as compared to other carcinomas of the lung (13,14). In terms of prognosis no differences between SCLC and LCNEC have been described. Because of the low incidence of this subtype, there is little information about specific prognostic or predictive markers (13,14).

Carcinoid tumors can be subdivided into typical and atypical carcinoids, which are, according to the recent WHO classification, defined as follows: Typical carcinoids have < 2 mitoses per 2 mm², lack necrosis, and measure ≥ 0.5 cm in size. Atypical carcinoids have 2-10 mitoses per 2 mm² and/or foci of necrosis. Relative to the high grade LCNEC and SCLC, typical carcinoids and atypical carcinoids are low- to intermediate-grade subtypes of lung neuroendocrine tumors, respectively (13,14). Patients with carcinoid tumors have a better prognosis and are usually younger than patients with other pulmonary neuroendocrine

tumors (23). Additionally, both carcinoid subtypes have very few genetic abnormalities compared with SCLC and LCNEC (24). Carcinoid tumors account for <1% of all lung cancers and occur more often in people who are female, white, or aged < 60 years. Interestingly, typical carcinoids are, in contrast to atypical carcinoids, not related to smoking (13,14).

1.1.3 Pathogenesis and molecular aspects

In many organs, including the lung, it has been demonstrated that cancer develops through a series of progressive lesions, which are typically called precursor or preneoplastic lesions. This multistep tumorigenesis corresponds with the accumulation of genetic and epigenetic changes (25,26). However, there are also studies suggesting that not a multistep, but rather a direct linear process is responsible for the development of malignant lung tumors (27,28). In fact, both above mentioned concepts could be compatible with each other, as different lung cancer subtypes presumably develop through different molecular pathways. The latter is substantiated by the variety of the different lung cancer subtypes regarding their cell of origin and anatomical location. For example, adenocarcinomas arise from small bronchi, bronchioles or alveolar epithelial cells and are typically located peripherally, whereas squamous cell carcinomas and SCLCs develop from the major bronchi and are located centrally in most cases (29). Therefore, the mechanisms of carcinogenesis will be discussed in the following for the three most common lung cancer subtypes separately:

In adenocarcinoma, the two most important signaling pathways involved in carcinogenesis are the epidermal growth factor receptor (EGFR) and Kirsten rat sarcoma viral oncogene (KRAS) pathways. Mutations in KRAS are associated with positive smoking status, whereas EGFR-mutations are linked to negative smoking status, East Asian ethnicity, and female gender (30–32). Atypical adenomatous hyperplasia most likely represents a preneoplastic lesion in the development of lung adenocarcinoma, as both entities share certain molecular alterations (33). For example, it could be demonstrated that up to 40% of atypical adenomatous hyperplasia lesions show KRAS mutations (34). Furthermore, atypical adenomatous hyperplasias express high levels of thyroid transcription factor 1 (TTF-1), a factor physiologically expressed in the lung periphery and terminal bronchioles, but also in the developing lung, where it is important for morphogenesis (35). In adenocarcinomas, the TTF-1 gene is often amplified, suggesting an oncogenic role of TTF-1 in this lung cancer subtype (36).

Squamous cell carcinomas develop through well-known precursor lesions: As a consequence of chronic tobacco smoke exposure, basal cells in the large airways give rise to metaplastic and dysplastic squamous cells. This process results in squamous cell dysplasia and carcinoma in situ (37). It has been demonstrated that these lesions show several molecular specificities. One such example is CDKN2A (p16), which acts as a tumor suppressor and is, by promoter region hypermethylation, inactivated in many tumor types. DNA methylation of CDKN2A is found in pulmonary squamous preinvasive lesions with, depending on histopathologic progression, increasing frequencies (17 % in basal cell hyperplasia, 24% in squamous metaplasia; 50% in carcinoma in situ) (38). Furthermore, the gene expression of vascular endothelial growth factor (VEGF) and its receptor (VEGFR) is, compared with normal bronchial epithelia, increased in squamous dysplastic lesions (39). The latter finding is consistent with a general principle of carcinogenesis: Tumor cells promote angiogenesis in response to a lack of oxygen supply, which in turn leads to an increase in vascular density (16). It has been demonstrated that SOX2, an oncogene that promotes survival and fosters the growth of tumor cells, is amplified in squamous cell carcinoma (40). At the protein expression level, it has been shown that SOX2 is completely absent in all phases of pulmonary adenocarcinoma pathogenesis, but is highly expressed in squamous cell carcinomas and in preinvasive squamous lesions of the lung (41). As on chromosome region 3q an amplification of SOX2 is only present in high-grade bronchial dysplasias but not in low-grade lesions, it can probably be assumed that SOX2 gets upregulated during pathogenesis of pulmonary squamous cell carcinoma (42). However, the earliest alterations in the sequence of squamous cell carcinoma pathogenesis already occur in normal-appearing bronchial epithelia, where allelic losses were described in several chromosome sites (3p12, 3p14, 3p21, 3p22-24, and 9p21) (43).

In SCLC, activation of the hedgehog pathway seems to play an important role in pathogenesis. As this signaling pathway is also required for normal lung development, it has been proposed that some types of SCLC might recapitulate some events of this physiological process (44). Further described genomic alterations in SCLC are amplifications in the FGFR1 oncogene, inactivation of TP53 and RB1, and mutations in PTEN, SLIT2, EPHA7, but also in the histone modifiers EP300, MLL, and CREBBP. Therefore, the authors of the mentioned study propose that histone modification is a major feature of SCLC (45).

In summary, recent developments in multiplex gene expression analysis and next-generation sequencing (NGS) technology provided many new insights into the molecular pathogenesis of lung cancer, some of which are already used in diagnosis and therapy. As a result, the current WHO classification of lung tumors incorporated some of these aspects in their molecular testing recommendations for treatment selection in lung cancer (46). However, in contrast to studies in malignant lung tumors, similar NGS studies in premalignant lung tissues have been very limited. Such studies would, according to a recent article by Kadara and colleagues (47), provide valuable insights into the earliest events that drive the pathogenesis of lung cancer and may also have implications for early detection and prevention efforts.

1.1.4 Diagnostic approach

In general, there are three possibilities how lung cancer can initially be found in a patient: incidentally in chest imaging, within a screening program, or because of occurring symptoms (48).

The symptoms of lung cancer can be classified according to tumor spread: Symptoms due to the location of the primary tumor in the lung comprise cough, dyspnea, haemoptysis, and wheezing. Symptoms due to local invasion or compression of adjacent structures are chest pain (resulting of pleural, chest wall, or mediastinal invasion), hoarseness (left recurrent laryngeal nerve), dysphagia, stridor, diaphragmatic paralysis (phrenic nerve), superior vena cava syndrome, or Pancoast syndrome (upper extremity muscle wasting, Horner, and shoulder pain). Symptoms as a result of distant metastasis include organ-specific symptoms of the brain, bone, liver, and adrenal gland. Constitutional symptoms (loss of appetite, weight loss, fatigue, and malaise) also belong to this category. Furthermore, in 10% of lung cancer patients, symptoms of a paraneoplastic syndrome occur: they comprise endocrine (e.g. hyponatraemia), musculoskeletal (e.g. hypertrophic osteoarthropathy), neurological (e.g. Lambert-Eaton myasthenia), haematological (e.g. anaemia), and dermatological (e.g. pruritus) symptoms (48,49).

In chest imaging, a pulmonary lesion is often found incidentally and without any accompanying symptoms. In most cases these lesions can be characterized as a non-calcified solitary pulmonary nodule (SPN). A SPN is defined as a solitary radiographic opacity with a diameter less than 3 cm on chest computed tomography (CT) scan. Furthermore, a SPN is not associated with intrathoracic lymph nodes or a pleural effusion and, with at least two thirds of its margins, is surrounded by normal lung parenchyma. If an SPN is detected, the further clinical evaluation is dependent on the appearance and size of the lesion, but also on the calculation of the pretest probability of malignancy. The latter is based on size, margin, cancer and smoking history, age, and location of the lesion. The combination of these parameters determines the further management of the nodule, e.g. follow-up CT or invasive procedures (48,50).

To date, the disease stage is the most important prognostic factor in lung cancer. Consequently, an adequate Tumor-Node-Metastasis (TNM) staging should be performed. Staging of lung cancer involves different imaging and endoscopic techniques: white light videobronchoscopy and autofluorescence bronchoscopy, CT scan (of chest and upper abdomen), cranial MRI (in Stage IB-III lung cancer), PET (complementary to CT; also integrated PET-CT available), and endosonography (48,49).

For an accurate pathological testing, clinicians must obtain tissue of sufficient quantity and quality from an appropriate tumor site. To achieve that in lung cancer, there are currently three main methods used: endoscopic biopsy, image-guided percutaneous core needle biopsy, and surgical biopsy. For endoscopic biopsy, many variants are available: endobronchial biopsy (forceps biopsy or cryobiopsy), transbronchial lung biopsy with or without guidance by radial endobronchial ultrasound (EBUS) miniprobe, EBUS-controlled transbronchial needle biopsy, oesophageal-guided fine needle aspiration, and thoracocentesis/ medical pleuroscopy. The image-guided (mostly CT- or ultrasound-guided) percutaneous core needle biopsy is used to obtain tissue from supraclavicular lymph nodes, from parenchymal or pleural nodes/masses and from liver or adrenal metastases. Video assisted thoracoscopy (VATS), a variant of surgical biopsy, is mainly used for diagnostic wedge resections and for the sampling of lymph nodes. Other variants of surgical biopsies comprise cervical mediastinoscopy and parasternotomy. Of all these techniques, the optimal one for the respective patient must be chosen. This decision should be based on the invasiveness and risk of a procedure, on the anticipated diagnostic yield and accuracy, on the accessibility of the respective site, and on the available local expertise (48,49).

1.1.5 Treatment of non-small cell lung cancer

Surgery in stage I and II NSCLC without mediastinal lymph node involvement includes the complete radical resection of the primary tumor. Additionally, a systematic mediastinal lymphadenectomy should be performed, as intraoperative staging becomes more precise. There are, depending on the functional status of the patient, several surgical principles to achieve the radical resection. They comprise sublobar resection, lobectomy, bilobectomy, and pneumonectomy. However, the role of sublobar resection, anatomical segmentectomy, or wide-wedge resection for early lung cancer is a subject of debate. The standard surgical treatment, at least for all tumors >2 cm and for tumors <2 cm that have a solid appearance on CT scan, is lobectomy with mediastinal lymph node dissection. After lobectomy, the morbidity rates vary from 3-6%. In these cases, prolonged air leak, recurrent nerve palsy, chylothorax, and bleeding are the typical complications. The most common approach to perform a lobectomy is via muscle-sparing anterolateral thoracotomy and is called open lobectomy. In contrast, video-assisted thoracoscopic surgery (VATS) lobectomy is a minimal-invasive procedure. VATS lobectomy for early-stage NSCLC is, in comparison to open lobectomy, associated with fewer postoperative complications, less postoperative pain, and a decreased length of hospital stay. Furthermore, the 5-year survival rate in stage IA NSCLC is near 80% both in open lobectomy and in VATS, indicating a similar clinical outcome with both procedures. However, it is recommended that patients should, in order to exclude locally advanced disease, undergo an accurate preoperative work-up, and that VATS lobectomy should only be performed at experienced centers (51). Another surgical technique, although restricted to centrally located tumors, is parenchyma-sparing sleeve resection. This technique can be performed to avoid pneumonectomy, while having an oncological outcome that is comparable to pneumonectomy or standard lobectomy (51).

In contrast to the clear-cut recommendations for surgery in Stage I and II NSCLC, the surgical treatment in stage III depends on the subclassification of the tumor. The latter comprises locally advanced primary tumors (T3N1, T4N0-1) and N2-positive NSCLC. In T3N1 and T4N0-1, radical resection can mostly be achieved. For patients who are not eligible for radical resection, an induction treatment can be applied before surgery in order to “down-stage” the tumor. For N2-positive NSCLC, there are no general treatment protocols due to the lack of evidence. However, at least in some studies, patients with N2 disease undergoing induction chemoradiotherapy and lobectomy had an improved

progression-free and overall survival compared to patients treated with chemoradiotherapy alone. Pneumonectomy can obtain favorable outcomes after induction chemoradiotherapy only, due to otherwise unusually high mortality, when performed at experienced centers (51).

In stage IV NSCLC, resection of both the primary and metastatic sites can be performed in combination with chemotherapy. However, careful patient selection is important, as only those patients are eligible in whom a complete resection of the primary tumor and continuous control of the distant metastatic sites are possible (51). In the palliative setting of patients with NSCLC, malignant pleural effusion is a terminal condition diminishing quality of life. Pleurodesis is mostly the treatment of choice in the management of malignant pleural effusion, but requires multiple hospital admissions and interventions. However, the latter could be reduced with the development of tunneled pleural catheters (TPCs). After the initial placement of a TPC, which requires two small incisions, patients can get their further treatment in outpatient care (51).

Radiotherapy is, in addition to surgery and drug treatment, a key modality in the treatment of lung cancer. It can be used both in the curative and in the palliative setting. In locally advanced NSCLC, concurrent radiotherapy and platinum-based chemotherapy is the standard of care in properly staged and fit patients. Typically, radiotherapy is delivered in doses of 2 Gy daily, with an overall dose in the range of 60-66 Gy. Side effects of radiotherapy comprise esophagitis, hematological toxicity, and radiation pneumonitis. Although the latter occurs in up to 30% of patients, it is very uncommon that those affected develop a fatal pneumonitis (52).

Chemotherapy regimens in NSCLC are mostly platinum-based and used in combination with other chemotherapeutic drugs. It has been shown that different combinations of this treatment modality are equally effective in terms of overall survival (53). Despite some clinical benefit, it seems that this chemotherapy has reached a plateau in metastatic NSCLC. In recent years, several new targeted therapies (including tyrosine kinase inhibitors, TKIs) and immunotherapies (including checkpoint inhibitors) have been developed. The European Society for Medical Oncology has already incorporated these new treatment options in their current Clinical Practice Guidelines (54).
EGFR TKIs currently comprise gefitinib, erlotinib, and afatinib. Compared with platinum-based chemotherapy these treatments result in improved progression-free survival and

response rate, especially in patients harboring activating EGFR mutations. Furthermore, patients treated with EGFR TKIs showed a superior quality of life and a better tolerance of the applied drug (54).

Crizotinib, an inhibitor of ALK, MET, and ROS1, is a very effective treatment option for patients harboring chromosomal rearrangements of ALK. However, due to the emergence of crizotinib resistance, the disease progresses in most patients within the first 12 months of treatment. These insights paved the way for the development of second-generation ALK inhibitors for crizotinib-resistant NSCLC. As ALK TKIs are now approved for first-line therapy, molecular testing should be performed in EGFR- and in ALK-genes simultaneously. In addition to second-generation ALK inhibitors, a number of alternative ALK inhibitors with broader activity against several mutated ALK genes are currently in clinical development (54,55).

Pembrolizumab and nivolumab are both monoclonal antibodies against the PD-1 receptor. In Europe, pembrolizumab is indicated as monotherapy for the first-line treatment of metastatic NSCLC in adults whose tumors express PD-L1 (the ligand of the PD-1 receptor) with a ≥50% tumor proportion score (TPS). Also, no EGFR or ALK tumor mutations should be present in these cases. The indication for pembrolizumab as second-line treatment of NSCLC in Europe is defined as follows: Locally advanced or metastatic disease in adults whose tumors express PD-L1 with a ≥1% TPS and who have received at least one prior chemotherapy regimen. EGFR or ALK positive tumors should have been treated with targeted therapy before receiving this second-line treatment (56). Nivolumab is indicated in Europe as monotherapy for the treatment of locally advanced or metastatic NSCLC in adults who have received prior chemotherapy (57). PD-1 receptor inhibitors belong to the ever-increasing group of immune checkpoint inhibitors. In general, immune checkpoints protect peripheral tissues from excessive immune responses and maintain self-tolerance. It is quite interesting that, despite lung cancer was historically seen as poorly immunogenic, NSCLC is now at the forefront of developments in cancer immunotherapy, a field considered to be the scientific breakthrough of the year 2013 (54,58).

1.2 The invasion-metastasis cascade

About 90% of all cancer-associated deaths are not caused by the primary tumor, but rather by metastasis. The latter is a multi-step process, often called the invasion-metastasis cascade. After the formation of the primary tumor, cancer cells have to invade the surrounding tissues, intravasate into and survive within the circulatory system, extravasate through the vascular wall into distant tissues, build micrometastatic colonies, and proliferate there in order to establish detectable metastatic lesions (59). This sequence of events is described in the following chapters chronologically.

1.2.1 Invasion and Intravasation

In the classical view (which will be further discussed and expanded later), the epithelial-mesenchymal transition (EMT) is seen as the very first step in the dissemination of carcinoma cells. This cell-biological program leads to the loss of epithelial features and the acquisition of properties associated with mesenchymal cells, including enhanced migratory capacity and invasiveness. To confirm a successful EMT experimentally, changes in the expression of epithelial and mesenchymal markers can be measured. For the epithelial phenotype, the most commonly used markers comprise E-cadherin, occludins, and cytokeratins. In contrast, N-cadherin and vimentin are mostly used to confirm a mesenchymal phenotype. Several EMT-inducing transcription factors are known to be responsible for the coordination of this process, e.g. Snail, Slug, Twist, and Zeb1 (60). Traditionally, the induction of the metastatic cascade has been viewed as being a late event during tumor progression (61). However, some studies have shown that EMT occurs, at least in certain cases, even in preneoplastic lesions, indicating that EMT (and possibly cancer cell dissemination) is a relatively early event (62).

After these first steps, the dissociated tumor cells invade the surrounding stroma and infiltrate vessels. Although both blood and lymphatic vessels can be invaded, it is presumed that draining lymph nodes represent dead ends for carcinoma cells. Therefore, the hematogenous transport of cancer cells is probably the main route of dissemination (63). Nonetheless, the spreading of tumor cells to draining lymph nodes is a valuable clinical parameter with prognostic relevance. For that reason, the histopathological regional lymph node status is well established in staging systems, including the TNM classification of malignant tumors (64). From a mechanistic point of view, it is likely that draining lymph nodes, although dead ends for cancer cells, function as surrogate markers that correlate with the extent of tumor cells disseminating into the blood circulation (63).

1.2.2 Circulation and Extravasation

Circulating tumor cells (CTCs) interact with many cell types during their intravascular journey to distant tissues, including platelets and neutrophils:

The association with platelets starts immediately after intravasation, because carcinoma cells express tissue factor on their cell membrane. This interaction can result in imbalances of the coagulation homeostasis, if many CTCs enter the circulation at the same time. Therefore, clotting symptoms, like disseminated intravascular coagulation, microthrombi, and pulmonary emboli, can occur in cancer patients (65). The contribution of platelets to the metastatic process is also highlighted by the fact that thrombocytopenia can have an anti-metastatic effect, which has already been proven experimentally in 1968 (66). Correspondingly, in most tumor types, including lung cancer, a high platelet count is associated with a poor prognosis in patients (67). The biological mechanisms behind these clinical associations are not yet fully understood. Still, in mice depleted of NK cells, the pro-metastatic effects of platelets are vanished. In the same study it was shown that thrombocytes can protect tumor cells from being eliminated by NK cells via deposition of fibrinogen and the formation of protective barriers around CTCs (68). This protection from NK-cells can not only be mediated by these mechanical shields but also by soluble factors, like TGF-ß (69). Another effect of platelets on tumor cells is the induction of EMT, which presumably facilitates the subsequent steps of metastasis (70).

Neutrophils elicit, under specific conditions, inhibitory effects on metastasis. One of these conditions is the secretion of CCL2 by tumor cells, a molecule which influences neutrophils in a way that they prevent cancer cells from building metastatic colonies in the lungs. This is achieved by accumulation of CCL2-primed neutrophils in the circulation and the lungs even before the progression of metastasis. In contrast, neutrophils treated with G-CSF, instead of CCL-2, cannot prevent lung metastasis (71). However, neutrophils can also facilitate cancer progression via neutrophil extracellular traps (NET). NETs are extracellular neutrophil-derived DNA webs with the ability to trap invading pathogens during an immune response. It has been shown that NETs can capture CTCs and, probably, increase their intraluminal survival, their adherence to endothelial cells, and their capacity to extravasate. Since NETs are released in response to inflammatory cues, this finding also provides an

explanation for the observation that severe postsurgical infection is associated with an adverse oncologic outcome (72). A well-known mechanism of neutrophils to promote metastatic spread is also immunosuppression. For example, it has been demonstrated that neutrophils can inhibit NK cells in their function of eliminating tumor cells. This leads to a significant increase in the intraluminal survival time of CTCs and, hence, increases their chances of building metastatic colonies (73).

For the extravasation of CTCs many different mechanisms have been described. One of them works via proliferation of carcinoma cells in the blood vessel lumen, leading to intraluminal tumor colonies. As these colonies continue to grow, they eventually rupture the vessel wall. This leads to direct access to the surrounding tissue, without the need to traverse the endothelial wall (74). Furthermore, it has been shown that tumor cell induced necroptosis (programmed necrosis) of endothelial cells can drive extravasation. This mechanism requires the interaction of the amyloid precursor protein on tumor cells with its receptor, death receptor 6 (DR-6), on endothelial cells. Therefore, it has been suggested that endothelial DR6-mediated necroptotic signaling pathways could be possible targets for anti-metastatic therapies (75). Platelets, in addition to their aforementioned interaction with CTCs, can also interact with endothelial cells and enable extravasation. In detail, tumor cell-activated platelets release adenine nucleotides which act on P2Y2 receptors of endothelial cells. This interaction induces the opening of the endothelial barrier and, consequently, allows transendothelial migration of tumor cells (76).

1.2.3 Colonization

After cancer cells have successfully extravasated into a distant tissue parenchyma, they often get eliminated immediately or enter a state of dormancy. In the latter, small tumor cell clusters or single tumor cells can persist for a very long time, sometimes even for years. This inefficiency to colonize distant organs after extravasation is principally determined by two distinct aspects of cell growth: failure of solitary cells to initiate growth, and failure of early micrometastases to continue growth into macroscopic tumors (77). The insufficiency in growth of disseminated tumor cells can have two reasons: On the one hand, they suffer from the lack of extracellular signals which they received when they were still part of the primary tumor in the tissue of origin. On the other hand, the tissue microenvironment in their new destination site is also rich of foreign signaling molecules which can initiate different responses, including a state of dormancy, in the disseminated tumor cells (78). For example, the extracellular matrix seems to play an important role in initiating dormancy programs, but also in providing mitogenic signals for the newly arrived tumor cells. In the lung, it was shown that the ability of disseminated tumor cells to interact with the matrix is dependent on the formation of filopodium-like protrusions that are coated with integrin ß1. In the absence of the latter, tumor cells fail to get proliferative signals from the extracellular matrix and, consequently, enter a dormancy state (79). Although the microenvironment provides many more dormancy-inducing factors, including TGF-ß2 in head-and-neck cancer (80) or BMP7 in prostate cancer (81), it seems that many of them activate the p38 MAPK pathway. This activation, in combination with missing mitogenic signals, leads to disseminated tumor cells with low ERK, and high p38 expression. The latter expression profile arrests cancer cells in the G0/G1 cell cycle phases, which are, in turn, associated with the state of tumor cell dormancy (82).

The founding of metastatic colonies relies on cells with the property of tumor initiation. Presumably, cancer stem cells (CSC) have this ability and are therefore the main drivers of colonization. In breast cancer, for example, it has been shown that CSCs are responsible for the initiation of lung metastasis. In the same study, enhanced Wnt signaling has been identified to be the major factor contributing to the maintenance of this stem cell population (83). Interestingly, activation of the previously mentioned EMT program can not only initiate mesenchymal traits, but also the expression of characteristic stem cell markers in carcinoma cells (84).

Taken together, these two mentioned studies provide evidence that there is probably a direct link between the EMT, the gain of stem cell properties, and the founding of metastatic colonies. However, comparing carcinoma metastases and their corresponding primary tumors, there are often similar histopathological patterns, including epithelial features, present in both tumor locations. These morphological findings seem to be incompatible with the idea that the EMT is a prerequisite to the founding of metastatic colonies. This paradox probably can be resolved by a mechanism that reverses the EMT after dissemination, which, consequently, is called Mesenchymal-Epithelial-Transition (MET). The MET restores most of the epithelial properties that were lost during the EMT, including cell-cell adhesions. Hence, this process provides an explanation for the complex multicellular growth patterns of metastatic lesions that can be observed during histopathological examinations (85).

From a mechanistic point of view, disseminated cancer cells must fulfill two requirements to build metastatic colonies. Apart from the above discussed ability to initiate tumor growth, which is attributed to CSCs, they also have to thrive in the microenvironment of the metastatic site. Basically, this idea has already been suggested in 1889 by Paget with his "seed and soil" hypothesis. There he stated that different types of tumor cells are distinct in their ability to build metastatic lesions in different types of tissue microenvironment:

> *(...) every single cancer cell must be regarded as an organism, alive and capable of development. When a plant goes to seed, its seeds are carried in all directions; but they can only live and grow if they fall on congenial soil* (86).

However, there have been, and still are, hypotheses claiming that tumor cells arrest nonspecifically in the first organ which they encounter after following the circulatory route from the primary tumor. For example, the liver is a common site of metastases for gastrointestinal tumors because of the portal venous system, which represents a unique venous drainage. Presumably, both the "seed and soil" and the anatomical/drainage hypotheses can coexist, as they do not have to be mutually exclusive and, furthermore, as it depends on the tumor type which of these mechanisms are predominant (87).

1.2.4 Emerging principles

In summary, all the above discussed mechanisms of the metastatic cascade are quite complex and sometimes contradictory. For that reason, Lambert et al recently suggested, referring to the famous “hallmarks of cancer” (61), a number of emerging biological principles of metastasis (88):

1) Metastasis occurs mainly through a sequential, multi-step process: the invasion-metastasis cascade.

2) Primary tumor cells, especially in carcinomas, accomplish most of the steps involved in the dissemination process by the help of an EMT.

3) During their transit through the circulatory system, metastasizing carcinoma cells experience many interactions with other blood components. These interactions influence the fate of the disseminating tumor cells.

4) Once disseminated, cancer cells must escape the attacks of immune cells. Furthermore, they have to subvert the state of dormancy, which is imposed by specific cellular programs.

5) The dissemination of cancer stem cells is a prerequisite of active metastatic colonization, because only this cell type can reinitiate tumor growth at distant sites. Additionally, the disseminated tumor cells or their progeny must have the ability to assemble colonization programs, which are organ-specific and adaptive. Furthermore, successful metastatic colonization depends on the establishment of a microenvironment that is advantageous to metastasis.

1.2.5 Approaches to study invasion and metastasis

Many of the recent advances in our understanding of the mechanisms leading to metastatic disease have their origin in the multiple experimental techniques which are available today. For example, the processes of collective invasion (an alternative mode of invasion, as opposed to single-cell invasion), can be studied both in vitro and in vivo by a variety of methods. In vitro, 2D and 3D time-lapse microscopy are the primary methods for monitoring collective cell migration. In 2D assays, the migration of confluent cells across a flat surface is studied, whereas in 3D assays also vertical migration across a 3D extracellular matrix scaffold can be observed. In vivo, collective invasion can be studied, for example, by intravital microscopy of tumor cells, by animal models, or by standard histological/ immunohistochemical analyses. The latter analyses can determine the extent of invasion and the presence of cell-cell junctions in migrating tumor cells. Additionally, the results of histological and immunohistochemical studies can be correlated with human pathology data. However, there is debate about whether in static 2D sections (without 3D reconstruction) cell groups disseminating as a cohort can be distinguished from single cells that subsequently proliferated (89,90). Furthermore, tumor cell budding, defined as the presence of small isolated tumor nests composed of less than 5 tumor cells in the stroma of the invasive tumor edge (91), cannot be reliably evaluated in 2D sections. A possible solution to overcome these limitations in 2D sections could be the use of already intravasated tumor cell clusters as a sign of successful collective invasion.

Migration and metastasis of tumor cells are regulated by a plethora of molecules. Using these molecules as markers and assessing their expression during the process of invasion could provide novel insights into the involved biological mechanisms. In the following, molecules related to these processes are described in terms of their physiological function, as well as in their (presumed) role in migration and metastasis.

Twist, ZEB, Snail, and Slug are transcription factors which are upregulated after the initiation of an EMT. These transcription factors decrease the expression of E-cadherin and increase the expression of vimentin and N-cadherin (92). Transforming growth factor-beta (TGF-ß) is a cytokine that has been described as a strong inducer of EMT (93).

E-Cadherin and N-Cadherin are transmembrane glycoproteins that mediate cell-cell-adhesion. Physiologically, they play important roles in tissue morphogenesis and homeostasis (94). However, cadherins are also involved in cancer progression. It has been shown in several tumor types that a switch from E-Cadherin to N-Cadherin expression is indicative of an EMT (95). Furthermore, E-Cadherin negatively regulates cell proliferation and migration in NSCLC via downregulation of RhoA or Cdc42 (96). In accordance with this finding, high expression of E-cadherin is positively correlated with the survival of NSCLC patients (97) .

Vimentin belongs to the protein family of intermediate filaments. Physiologically, vimentin is expressed predominantly in mesenchymal cells, while an overexpression has also been described in many epithelial cancers (98). In this context, vimentin is regarded as a marker for a successful EMT (60). In the normal adult bronchial epithelium, its expression is limited to basal and columnar cells (99). In NSCLC, vimentin is widely expressed in tumor cells (100) and correlates with poor survival of patients (97).

Brk, mad, rack1, and sax are genes recently described to be related to border cell migration in drosophila melanogaster. As drosophila border cells migrate predominantly via collective cell migration, they provide a powerful model to study also the process of human collective cancer cell invasion (101).

Rab40B and Tks5 were both described to be involved in the formation of invadopodia (102–104). Invadopodia (present in cancer cells) and podosomes (present in normal cells) are dynamic protrusions of the plasma membrane. As both structures share major biological features (e.g. the ability to degrade and remodel the extracellular matrix), they are sometimes collectively called “invadosomes” (105).

Fascin1 regulates the stability and maintenance of filamentous actin bundles and is involved in many cellular mechanisms, including cell adhesion, migration, and invasion (106). It is expressed mainly in neuronal cells, smooth muscle cells, endothelial cells, fibroblasts, and, interestingly, also in motile embryonic cells. In contrast, there is only a low expression or even an absence of fascin1 in normal epithelial tissue (107). In malignant epithelial tissue, however, fascin1 is often highly expressed. In this context, fascin1 has been described as a prognostic marker in colorectal, esophageal, breast, and head and neck squamous cell carcinomas (108). Presumably, fascin1 promotes the invasion of tumor cells via stabilization of actin bundles in invadopodia (109).

ERK1 and ERK2 are part of the Ras-Raf-MEK-ERK signaling pathway. This pathway is involved in the regulation of many cellular processes, including cell migration, proliferation, differentiation, and cell adhesion. ERK1 and ERK2 get activated via phosphorylation of both tyrosine and threonine. Activated ERK1/2 catalyzes the phosphorylation of nuclear transcription factors, which requires the translocation of ERK1/2 into the nucleus (110). About one-third of all human cancers show an increased activity of the Ras-Raf-MEK-ERK cascade (110), including NSCLC (111). Phospholipase C gamma (PLCγ) is an important factor especially during development, for example as a downstream signaling molecule of the VEGF-receptor during development of arterial vessels (112). Furthermore, PLCγ probably has a major role in integrin-mediated cell motility processes (113). An association of PLCγ with cancer cell invasion has also been described (114).

RhoA and CdC42 both belong to the family of Rho GTPases. When bound to GTP, this protein family is active, and when bound to GDP, it is inactive. Rho GTPases are essential for many cellular mechanisms, including both single and collective cell migration (115). In cancer, both RhoA (116) and CdC42 (117) seem to be pro-tumorigenic. This is in accordance with results of the above mentioned study in NSCLC, which links E-Cadherin with RhoA and CdC42 (96).

Connexins are the essential part of gap junctions (cell-cell contacts) and hemichannels (cell-ECM contacts). Therefore, they are very important for all kinds of biological processes which involve intercellular communication, both in health and disease (118). In cancer progression, connexins have a mostly tumor suppressive role in early stages, and a mostly

tumor promotive role in advanced stages. However, these general principles do not always apply, as there are 21 different connexins in the human genome (118). More specifically, it has been suggested that connexin43 is probably a marker of tumor vasculature and micrometastases (119). In NSCLC, overexpression of connexin43 has been shown to reverse EMT and cisplatin resistance (120).

Chemokines are cytokines that mediate cell migration in a directed (chemotactic) way. The term chemokine (chemotactic cytokine) derives from these two characteristics. Chemokines bind to G-protein coupled receptors and can be classified into the following subgroups: CXC, CC, CX_3C, and C chemokines (121). The function of chemokines is best understood in leukocytes, where they regulate different steps of the immune response, including cell trafficking (122). It is estimated that there are about 50 different chemokines and 20 different chemokine receptors in humans (123). Many of them have been described to play an important role in the pathogenesis of cancer, including metastasis (123). For example, CXCR1 and its ligand CXCL8 (also known as IL8) are involved in the induction of EMT in carcinoma cells (124). For CXCR2, it has been demonstrated that its expression on tumor cells promotes the invasion-metastasis cascade and is a poor prognostic factor in NSCLC (125). Furthermore, CXCR2 is probably implicated in the process of inflammation-driven tumorigenesis (126). CXCR4 is overexpressed in at least 23 different human cancer types and contributes to many steps of tumor progression, including invasion and metastasis (127). In NSCLC, a high expression of CXCR4 is associated with a worse overall survival (128) and with brain-specific metastasis (129).

SMARCA4/BRG1 is a key factor in SWI/SNF chromatin remodeling complexes. The latter can modulate chromatin structure and are involved in a plethora of cellular processes, such as DNA repair, cell cycle control, and differentiation. Taken together, SWI/SNF chromatin remodeling complexes are mutated in 20% of all human cancers (130). In NSCLC, SMARCA4 inactivation alters nucleosome positioning and is associated with a higher aggressiveness of the tumor (131). However, it has also been shown that SMARCA4 deficiency in NSCLC correlates with a differentiated histological phenotype (132) and with an increased sensitivity to platinum-based chemotherapy (133).

2 AIM OF THE PRESENT STUDY

Histopathological findings question the current doctrine that an EMT is indispensable for invasion and metastasis: Instead of migrating as separated single cells, which would be the logical consequence of a complete EMT-program, carcinomas rather move as multicellular complexes. In lung malignancies, this collective way of migration seems to be most frequently occurring in adenocarcinomas, squamous cell carcinomas, and large cell carcinomas. Despite the commonness of collective cell migration in cancer, relatively little is known about the actual mechanisms behind these morphological findings.

Therefore, the aim of our retrospective study was to further examine this mode of cell migration in NSCLC patient samples by immunohistochemistry. More specifically, we wanted to evaluate the expression and distribution of classical EMT-markers and of other molecules associated with migration and metastasis.

3 MATERIALS AND METHODS

To achieve the above-mentioned study aim, we used tissue specimens from 558 NSCLC patients (30 for the study set and 528 for the validation set). All patients gave their written informed consent. Our study was approved by the ethics committee of the Medical University of Graz (No. 24-135).

3.1 Study set

3.1.1 Tissue acquisition and selection criteria

All selected histopathological cases of the study set were obtained from NSCLC patients who had undergone thoracic surgery between 2011 and 2012. Depending on the performance status of the respective patient, sublobar resection, lobectomy, bilobectomy, or pneumonectomy had been performed. The resulting surgical specimens had been processed, fixed in 4% neutral-buffered formalin, and paraffin-embedded according to the standard protocols of the Institute of Pathology, Medical University of Graz. Subsequently, the formalin-fixed, paraffin-embedded (FFPE) tumor tissue samples had been stored at the Lung Archive of the same institution.

At the beginning of our study, 30 cases of NSCLC with clear vascular invasion were retrieved from the Lung Archive. To avoid a staining bias later on, the selected FFPE tissue samples had to have the central tumor, the invasion front (to lung or pleura), and the vascular invasion site on the same tissue slide. To verify these morphological criteria, 4 µm thick sections of the FFPE blocks were deparaffinized with xylol, dehydrated via a graded ethanol series of increasing ethanol concentrations, and stained with Hematoxylin-Eosin (H&E). These steps were carried out by qualified technicians of the Laboratory of Histology at the Institute of Pathology, Medical University of Graz. The H&E tissue sections were evaluated by Prof. Dr. Helmut H. Popper and only those 30 cases that have met the above-mentioned criteria were included in the study set.

3.1.2 Study population

The 30 selected cases (patient characteristics are shown in Table 1) comprised 17 adenocarcinomas (56.7%), eight squamous cell carcinomas (26.7%), and two large cell carcinomas (6.7%). Three cases (10.0%) had an ambiguous histopathological diagnosis and were classified as mixed types of NSCLC. The population of the study set had a median age of 65 years (range of 47-73). In terms of gender distribution, the 30 cases consisted of 9 women (30.0%) and 21 men (70.0%). In 29 cases (96.7%) the smoking status was known and showed a clear preponderance of current- or ex-smokers (together 83.3%). Only four patients (13.3%) had no smoking history at all. Due to our selection criteria, all cases of the study set were characterized by vascular invasion (V1). Further histopathological details about tumor size (T), lymph node metastases (N), and grading (G) are provided in Table 1.

Table 1: Patient characteristics of the study set (n = 30) at the time of surgery / pathological diagnosis

Characteristic	**Categories**	**N (%)**
Age	Median	65
	Range	47-73
Gender	Female	9 (30.0%)
	Male	21 (70.0%)
Smoking status	Current-smoker	13 (43.3%)
	Ex-smoker	12 (40.0%)
	Never-smoker	4 (13.3%)
	No data available	1 (3.3%)
Histological type	Adenocarcinoma	17 (56.7%)
	Squamous cell carcinoma	8 (26.7%)
	Large cell carcinoma	2 (6.7%)
	Others (e.g. mixed types)	3 (10.0%)
Tumor size	T1a	1 (3.3%)
	T1b	3 (10.0%)
	T2a	15 (50.0%)
	T2b	7 (23.3%)
	T3	4 (13.3%)

Lymph node metastases	N0	12 (40.0%)
	N1	15 (50.0%)
	N2	2 (6.6%)
	NX	1 (3.3%)
Vascular invasion	V0	0 (0%)
	V1	30 (100%)
Grading	G1/G2	1 (3.3%)
	G2	8 (26.7%)
	G2/G3	7 (23.3%)
	G3	14 (46.7%)

3.1.3 Sample preparation and immunohistochemical staining

To immunohistochemically evaluate the 30 selected cases, 4 µm thick sections of the FFPE blocks were deparaffinized with xylol and dehydrated via a graded ethanol series of increasing ethanol concentrations. Depending on the used antibody, the tissue sections were pretreated with different antigen retrieval protocols. In Table 2 (chapter 3.3 “Primary Antibodies”), the pretreatment procedures for all used antibodies are summarized.

The selection of the used antibodies was based on a literature search for molecules that are related to cell migration and invasion. Consequently, 30 purchased antibodies were incubated with the individually pretreated tissue sections in accordance with the standard protocols of the Institute of Pathology, Medical University of Graz, and with the specifications of the respective manufacturers. Each of the 30 used antibodies is listed in Table 2 with details about the manufacturer, dilution, pretreatment, and detection.

The tissue sections as well as the immunohistochemical staining procedures and controls were carried out by BMA Sylvia Eidenhammer, Laboratory of Immunohistochemistry, Institute of Pathology, Medical University of Graz.

3.1.4 Interpretation of immunohistochemical staining

In the study set, all 30 markers were evaluated in terms of their staining pattern, intensity, extent, and, according to the above described selection criteria, distribution. Because of the latter, we could compare the expression profile of each marker between the tumor center, the invasion front, and the vascular invasion site. The criteria for staining positivity and staining intensity were established by an experienced pulmonary pathologist, Prof. Dr. Helmut H. Popper. To be regarded as positive, at least 1% of the tumor cells had to be stained.

3.2 Validation set

To avoid a selection bias and because the study set comprised only 30 cases, we validated the expression of the tested molecules in a larger cohort of NSCLC (n=528). We chose the tissue microarray (TMA) technology, because it allows the use of a single immunohistochemical staining protocol in a large patient cohort and therefore reduces staining variability. Also, the small amount of tissue that is needed for the preparation of TMAs makes this technique a good choice for precious pathological specimens (134–136).

3.2.1 Tissue acquisition and selection criteria

The 528 histopathological cases of the validation set were obtained from NSCLC patients who had undergone thoracic surgery between 1992 and 2012. The surgical and subsequent pathological approach was basically the same as in the cases of the study set.

The selected cases of the validation set (325 cases of AC, 142 cases of SCC, and 61 cases of LC) were also retrieved from the Lung Archive at the Institute of Pathology, Medical University of Graz. In contrast to the rigorous selection criteria in the study set (central tumor, invasion front, and vascular invasion site all on the same tissue slide), the only prerequisite for inclusion in the validation set was a confirmed histopathological diagnosis of NSCLC.

3.2.2 Tissue microarray preparation and immunohistochemical staining

At least 3 cores of tumor tissue and 1 core of normal lung tissue (each with a diameter of 0.6 mm) were punched from the same tissue block (donor block). Each core was subsequently assembled into another paraffin block (recipient block). For these steps, a manual TMA instrument (Beecher Instruments Inc, Sun Prairie, WI, USA) was used. Figure 17 and Figure 18 show exemplary histological sections (both are IHC stainings for pERK) of a donor block and of a recipient block.

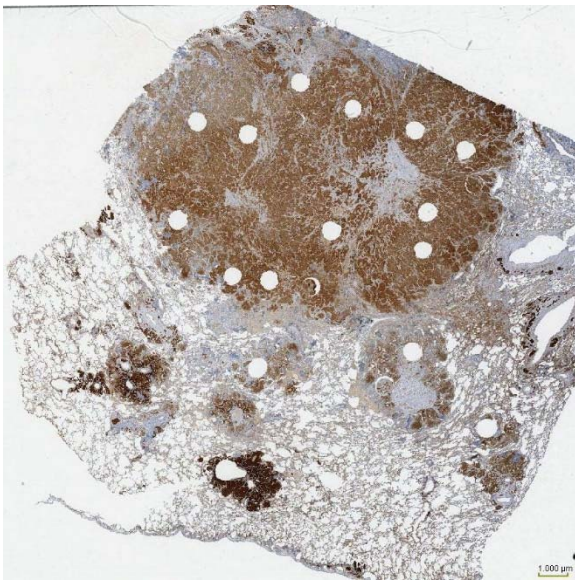

Figure 17: Histological section of a TMA donor block; IHC staining pERK; Scale bar 1000µm

Figure 18: Histological section of a (partial) TMA recipient block; IHC staining pERK; Scale bar 1000µm

From these TMA donor blocks, 4 µm thick sections were cut. These sections were then deparaffinized, dehydrated, and pretreated for antigen retrieval using the same procedures as described above for the study set.

In the validation set, immunohistochemistry was only performed for markers which showed differences in staining patterns between the central tumor part and the invasion sites (invasion front and/or vascular invasion) in the study set. Consequently, the markers Connexin43, Mad, Twist, Vimentin, PLCγ, Tks5, E-Cadherin, N-Cadherin, and pERK were included in the validation set. The incubation of these 9 antibodies with the pretreated TMA tissue sections was done in the same way as in the study set. In Table 2, each of the 9 used antibodies is listed with details about the manufacturer, dilution, pretreatment, and detection.

The tissue microarray preparation and section, as well as the immunohistochemical staining procedures and controls were performed by BMA Sylvia Eidenhammer, Laboratory of Immunohistochemistry, Institute of Pathology, Medical University of Graz.

3.2.3 Interpretation of immunohistochemical staining

To evaluate the expression profile of the 9 selected markers immunohistochemically, either the staining extent (for Connexin43, Mad, Twist, Vimentin, PLCγ, and Tks5) or the staining intensity (for E-Cadherin, N-Cadherin, and pERK) was assessed within the tumor tissue. For the staining extent, the percentage (0-100%) of positive tumor cells was assessed. All cases with a staining extent of at least 1% were defined as positive. For the assessment of the staining intensity, a scoring system (0-2) was used: 0 = no staining; 1 = weak to moderate staining; 2 = strong staining. All cases with a staining intensity score of 1 or 2 were defined as positive. In contrast to the study set, the staining distribution could not be evaluated in the validation set due to the spatial limitations of TMAs. Therefore, the expression profile of the respective marker could here not be compared between the tumor center, the invasion front, and the vascular invasion site.

3.3 Primary Antibodies

Table 2: Overview of the tested molecules and the used antibodies. Dilution, pretreatment, and visualization procedures are also shown.

Marker	Company	Dilution[1]	Pretreatment[2]	Visualization[3]
Brk	Biosource	1:200	CC1mild	UV/DAB
CdC42	Santa Cruz	1:50	MW 6.0	ENV/DAB
Connexin43	Novusbio	1:500	CC1mild	UV/DAB
CXCR1	Abcam	1:200	MW 9.0	ENV/DAB
CXCR2	Abcam	1:200	MW 9.0	ENV/DAB
CXCR4	Abcam	1:500	WB 6.0	HRP/DAB
E-Cadherin	Dako	rtu	high pH	Omnis Flex
ERK1/2	Cellsignaling	1:100	MW Tris	ENV/DAB
FAK	Abcam	1:1000	MW 6.0	ENV/DAB
Fascin 1	Chem	1:500	MW 6.0	CM/AEC
ILK	Abcam	1:100	CC1mild	UV/DAB
Mad	Novusbio	1:100	CC1mild	UV/DAB
N-Cadherin	Abcam	1:500	CC1mild	UV/DAB
PLCγ	Abcam	1:100	MW 9.0	ENV/DAB
Rab40B	Proteintech	1:200	MW 6.0	ENV/DAB
Rack1	Spring	1:100	CC1mild	UV/DAB
RhoA	Abcam	1:200	MW 6.0	ENV/DAB
SARI	Novusbio	1:200	CC1mild	UV/DAB
SAX	Abcam	1:200	CC1mild	UV/DAB
Slug	Novusbio	1:100	CC1mild	UV/DAB
SMARCA4	Abcam	1:200	CC1mild	UV/DAB
Snail	Santa Cruz	1:50	MW 6.0	ENV/AEC
pSRC	Abcam	1:100	CC1mild	UV/DAB
TGFß1	Santa Cruz	1:50	CC1mild	UV/DAB
Tks5	Novusbio	1:75	MW 6.0	ENV/DAB
Twist	Novusbio	1:50	MW 6.0	ENV/DAB
Vim	Dako	rtu	low pH	Omnis Flex

YAP	Abcam	1:300	CC1mild	UV/DAB
ZEB1	Abcam	1:200	CC1mild	UV/DAB
ZFPL1	Abcam	1:200	CC1mild	UV/DAB

1) Abbreviations: rtu = ready-to-use

2) Abbreviations: CC1mild = Cell Conditioning 1 Solution, Ventana; MW = microwave; WB = water bath; 6.0 = Target Retrieval Solution, pH 6.0, Dako; 9.0 = Target Retrival Solution, pH 9.0, Dako; Tris=TrisHCl + 5% Urea, pH 9.5; high pH = Target Retrieval Solution, High pH (Dako Omnis); low pH = Target Retrieval Solution, Low pH (Dako Omnis)

3) Abbreviations: ENV/DAB = ChemMate DAKO EnVision Detection Kit, Peroxidase/DAB, Rabbit/Mouse, Dako; UV/DAB = ultraView Universal DAB Detection Kit, Ventana; HRP/DAB = EnVision+ System-HRP (DAB), Dako; Omnis Flex = EnVision Flex (Dako Omnis); CM/AEC = ChemMate Detection Kit Peroxidase/AEC, Mouse/Rabbit, Dako; ENV/AEC = EnVision+ System-HRP (AEC), Dako

4 RESULTS

4.1 Study set

All 30 markers were evaluated in terms of their staining profile in the 30 resection samples of lung tissue (Table 3). In the following, each marker will be discussed separately.

Table 3: Comparison of positive marker expression between the tumor center (TC), the invasion front (IF), and the vascular invasion site (VI) in the study set (n = 30). The respective staining patterns are also shown: nuclear (nuc), cytoplasmic (cyt), and membranous (mem).

Marker	Positive in TC[1] N (%)	Positive in IF[1] N (%)	Positive in VI[1] N (%)	Staining pattern[2]
Twist	30 (100%)	30 (100%)	30 (100%)	nuc, cyt
ZEB1	1 (3.3%)	1 (3.3%)	1 (3.3%)	nuc
Snail	13 (43.3%)	13 (43.3%)	13 (43.3%)	nuc, cyt
Slug	0 (0.0%)	0 (0.0%)	0 (0.0%)	-
TGFß1	0 (0.0%)	0 (0.0%)	0 (0.0%)	-
E-Cad	30 (100%)	30 (100%)	30 (100%)	mem
N-Cad	30 (100%)	30 (100%)	30 (100%)	mem
Vim	0 (0.0%)	9 (30.0%)	9 (30.0%)	cyt
Mad	23 (76.7%)	23 (76.7%)	23 (76.7%)	nuc, cyt
Brk	15 (50.0%)	15 (50.0%)	15 (50.0%)	nuc, cyt
SAX	0 (0.0%)	0 (0.0%)	0 (0.0%)	-
Rack1	0 (0.0%)	0 (0.0%)	0 (0.0%)	-
Rab40B	0 (0.0%)	15 (50.0%)	15 (50.0%)	nuc, cyt
Tks5	0 (0.0%)	21 (70.0%)	21 (70.0%)	cyt, mem
Fascin 1	19 (63.3%)	26 (86.7%)	26 (86.7%)	cyt
pERK1/2	10 (33.3%)	16 (53.3%)	16 (53.3%)	nuc, cyt
PLCγ	0 (0.0%)	22 (73.3%)	22 (73.3%)	cyt
RhoA	27 (90.0%)	27 (90.0%)	27 (90.0%)	cyt
CdC42	2 (6.7%)	5 (16.7%)	5 (16.7%)	cyt, mem
Connexin43	20 (66.7%)	20 (66.7%)	20 (66.7%)	cyt, mem
CXCR1	30 (100.0%)	30 (100.0%)	30 (100.0%)	cyt
CXCR2	11 (36.7%)	11 (36.7%)	11 (36.7%)	nuc, cyt

CXCR4	9 (30.0 %)	9 (30.0 %)	9 (30.0 %)	cyt, mem
FAK	15 (50.0%)	15 (50.0%)	15 (50.0%)	cyt
ILK	18 (60.0%)	18 (60.0%)	0 (0.0%)	nuc, cyt
p-SRC	6 (20.0%)	4 (13.3%)	0 (0.0%)	nuc
SARI	0 (0.0%)	0 (0.0%)	0 (0.0%)	-
SMARCA4	30 (100.0%)	30 (100.0%)	30 (100.0%)	nuc
YAP	29 (96.7%)	29 (96.7%)	29 (96.7%)	nuc, cyt
ZFPL1	8 (26.7%)	0 (0.0%)	0 (0.0%)	nuc, cyt

1) Abbreviations: TC = tumor center; IF = invasion front; VI = vascular invasion site

2) Abbreviations: nuc = nuclear; cyt = cytoplasmic; mem = membranous

The EMT-inducing transcription factors Twist, ZEB1, Snail, and Slug were stained as follows: All cases (30/30) were characterized by nuclear positivity for Twist, without any differences between the tumor center, the invasion front, and the vascular invasion site (Figure 19). The staining intensities for Twist varied from moderate to strong, and in some cases an additional cytoplasmic staining was present. In contrast, only one case (1/30) was positive for ZEB1 and showed a nuclear staining pattern. Snail was positive in 13/30 cases (nuclear and cytoplasmic), although only in a few cells with minimal intensity. Slug was not expressed at all (0/30). TGFß1, an EMT-inducing cytokine, was also negative in all cases (0/30).

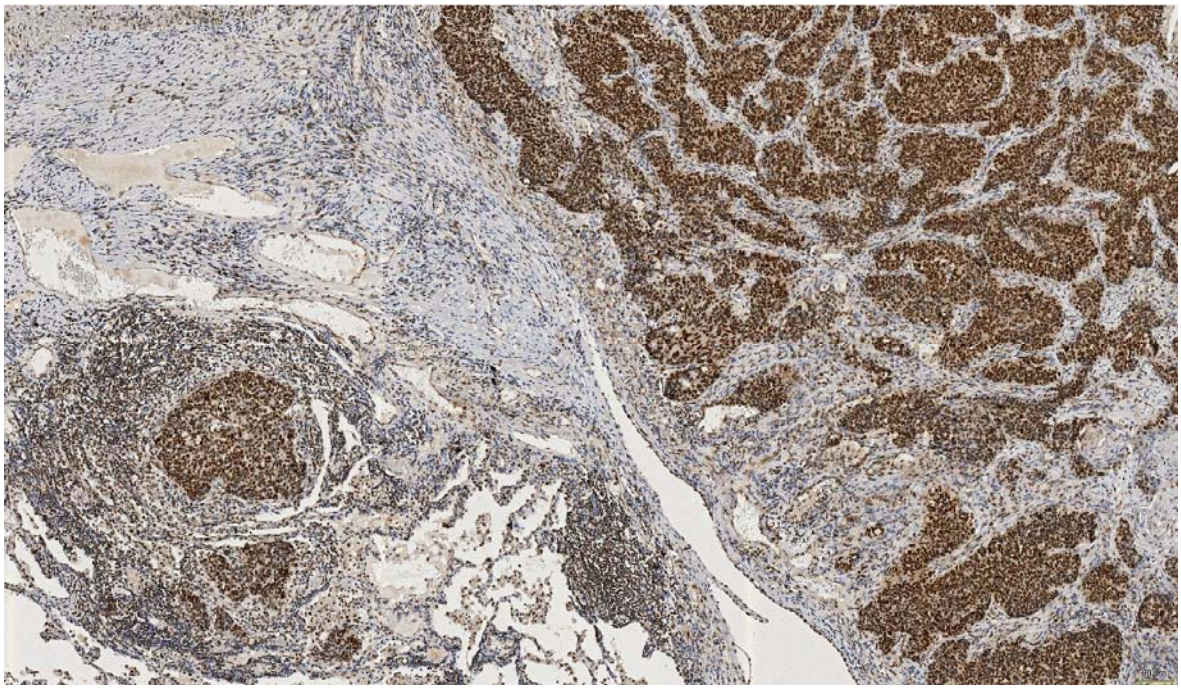

Figure 19: IHC Twist with nuclear staining pattern. The vascular invasion site (on the left) shows a similar staining intensity as the main tumor (on the right). Scale bar 90 µm

Markers for EMT were stained as follows: E-cadherin was positive in all tumors (30/30) and showed a classical membranous staining pattern. However, the intensity varied remarkably: In 24/30 cases, the invasion front and the vascular invasion site were less intensely stained compared to the tumor center (Figure 20). In some cases (8/30), there was a loss of E-cadherin in a few cells within the tumor bulk. N-cadherin was also positive in all tumors (30/30; membranous staining pattern), with 9/30 cases demonstrating a stronger intensity than the remaining cases. In 9/30 carcinomas, vimentin was only positive in several tumor cells (cytoplasmic staining pattern; Figure 21) at the invasion front and in the blood vessels, whereas in the tumor center there were no (0/30) vimentin positive tumor cells at all. The vimentin positive tumor cells at the invasion sites were still connected to the main tumor cell bulk. They showed no or only a reduced E-cadherin positivity. In 21/30 cases, vimentin was neither expressed at the tumor center nor at the invasion sites.

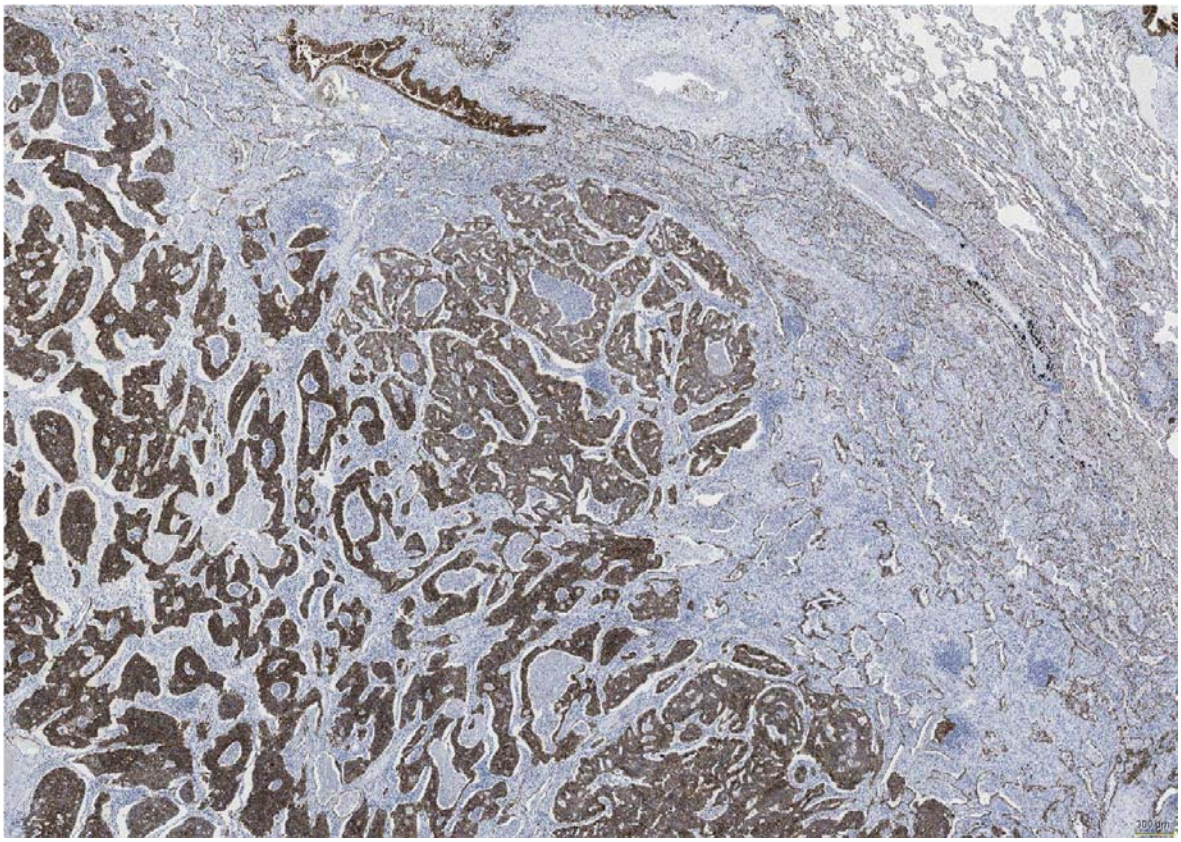

Figure 20: IHC E-cadherin with membranous staining pattern. The tumor center (bottom/left) is more intensely stained than the invasion front (in the middle). For spatial orientation, non-tumorous lung tissue is shown (top/right). Scale bar 300 µm

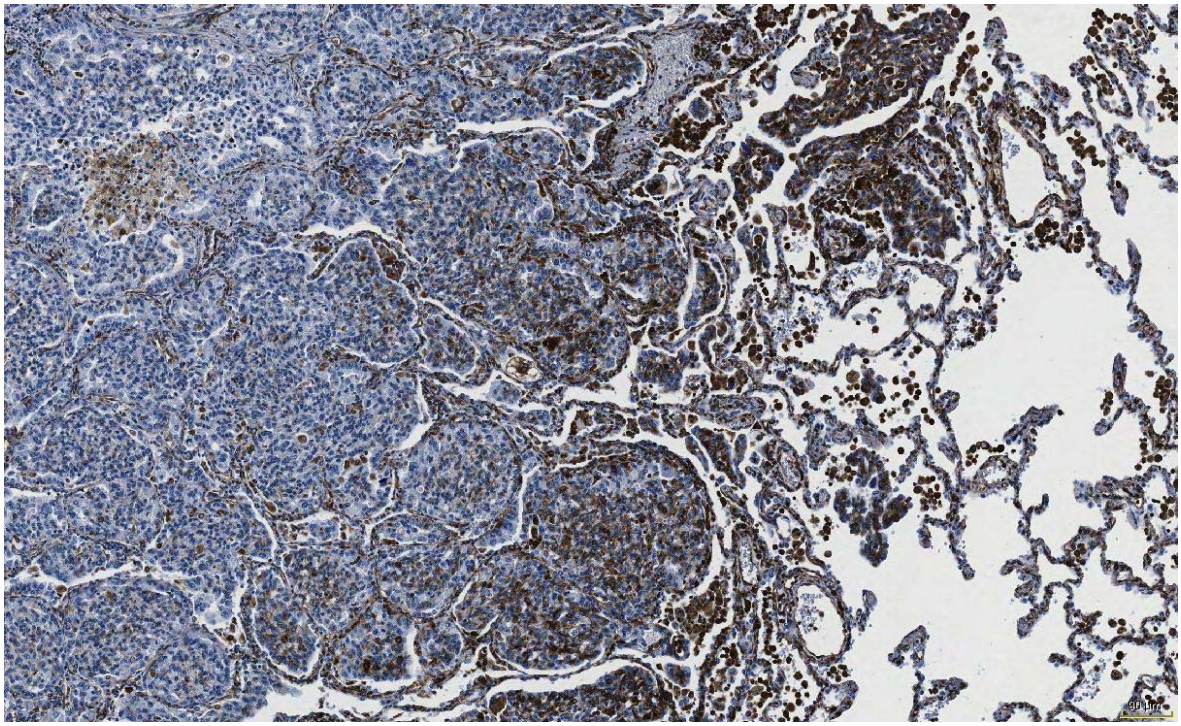

Figure 21: IHC Vimentin with cytoplasmic staining pattern. The tumor center (on the left) is Vimentin-negative, wheras the invasion front (in the middle) is Vimentin-positive. For spatial orientation, non-tumorous lung tissue is shown (on the right). Scale bar 90 µm

Molecules described as being important for border cell migration in Drosophila were stained as follows: Mad was positive in 23/30 cases, Brk was focally positive in 15/30 cases (Figure 25 on the next page). Both markers showed a nuclear and cytoplasmic staining pattern. Neither in Mad nor in Brk there were any differences in the number of positive cases between the tumor center, the invasion front, and the vascular invasion site. However, the invasion sites were usually stained more intensely. Interestingly, all carcinomas positively stained for Brk (15/30) were also positive for Mad. In contrast, SAX and Rack1 were negative in all cases.

Markers associated with invadopodia formation and stabilization were stained as follows: Rab40B demonstrated nuclear and cytoplasmic positivity in 15/30 tumors. Tks5 was positive in 21/30 tumors with a cytoplasmic and membranous staining pattern. Rab40B (Figure 23) and Tks5 (Figure 24 on the next page) were both almost exclusively stained at the invasion front and at the vascular invasion site. Rab40B was coexpressed with Tks5 in 11/15 cases. Interestingly, all Tks5 positive carcinomas were also positive for Mad.

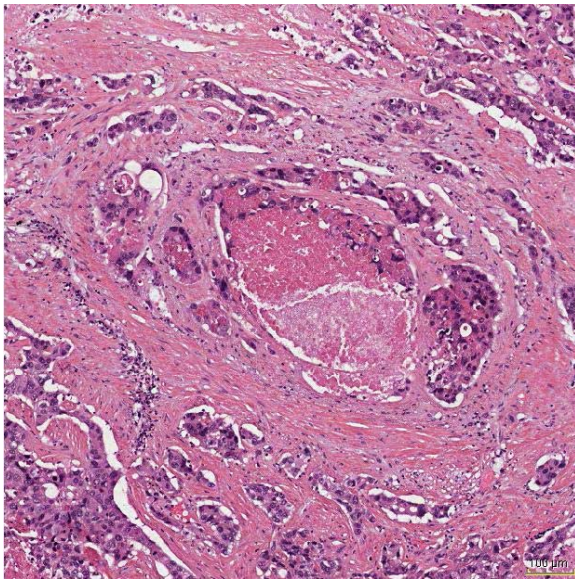

Figure 22: HE-staining of a vascular invasion site. Tumor cell clusters are assembled around a blood vessel and have already invaded the vessel wall and lumen. Scale bar 100 µm

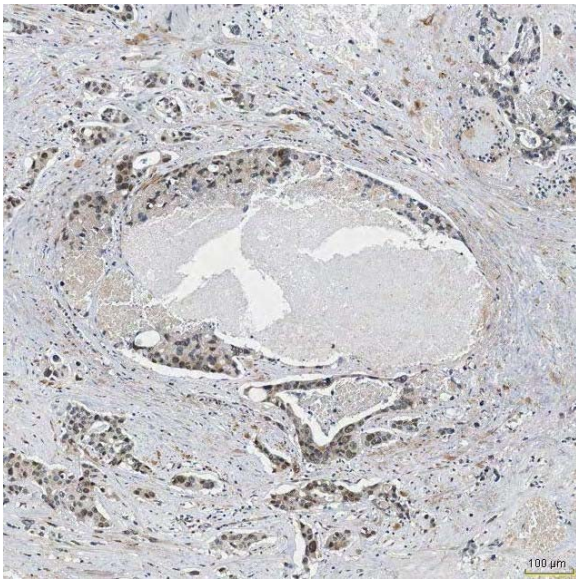

Figure 23: IHC Rab40B with nuclear and, here to a lesser extent, cytoplasmic staining pattern of the same vascular invasion site as in Figure 22. Scale bar 100µm

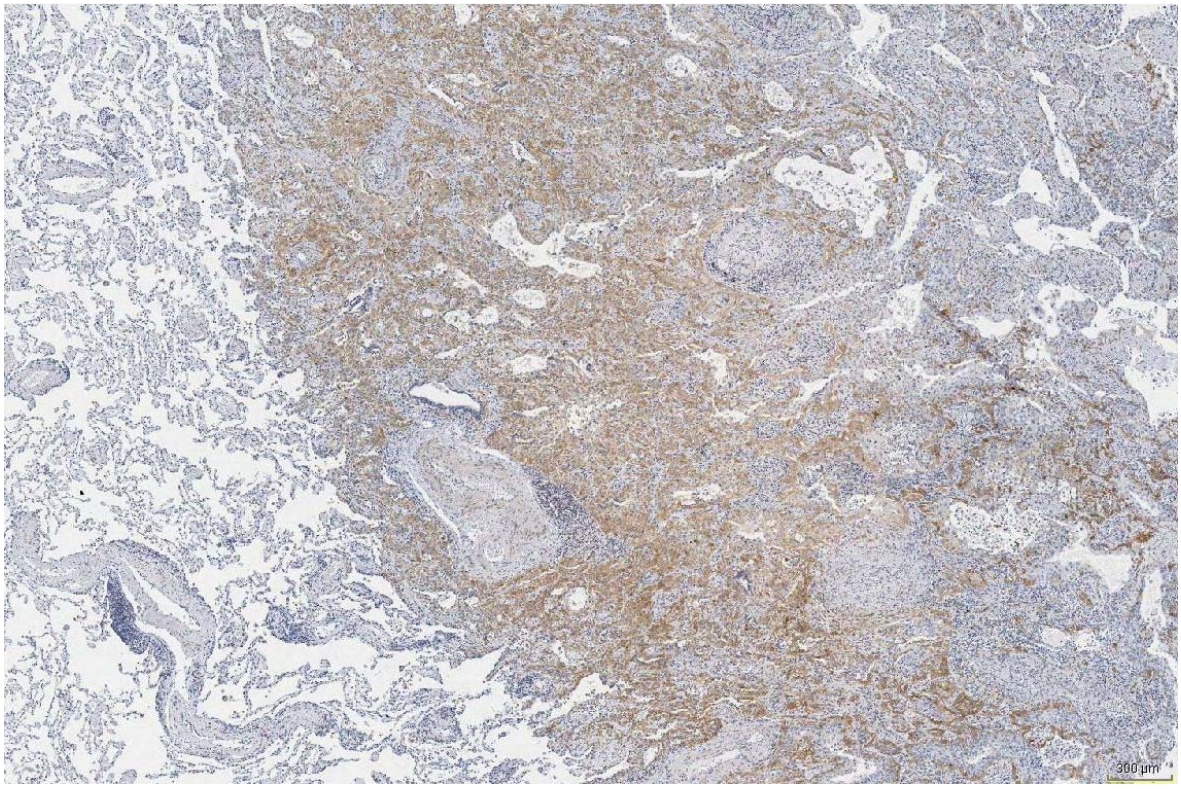

Figure 24: IHC Tks5 with cytoplasmic and membranous staining pattern of the same resection specimen and region as the figure below (Figure 25). The invasion front (in the middle) is Tks5-positive, wheras the tumor center (on the right) is Tks5-negative. For spatial orientation, non-tumorous lung tissue is shown (on the left). Scale bar 300 µm

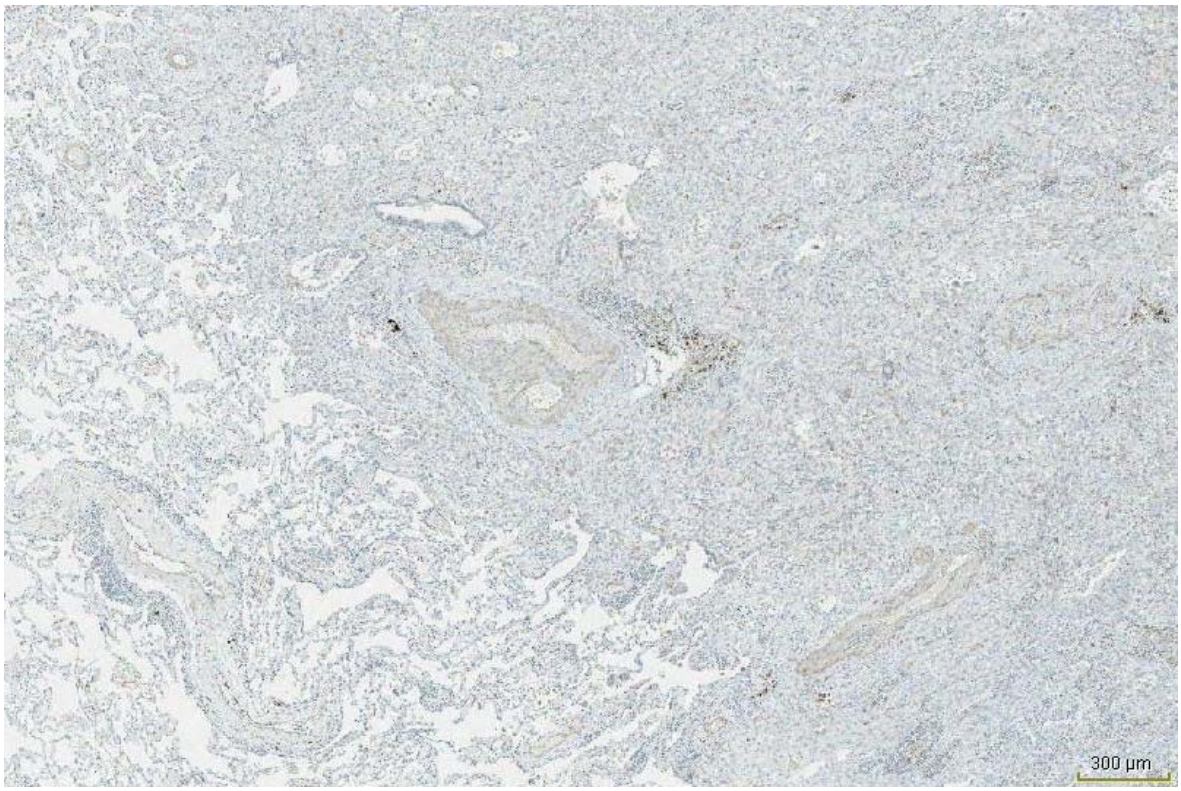

Figure 25: IHC Brk with nuclear and cytoplasmic staining pattern of the same resection specimen and region as the figure above (Figure 24). Brk-positive tumor cells are scattered across the tumor (on the right) with low staining intensity. There are no differences in staining intensity within the tumor. For spatial orientation, non-tumorous lung tissue is shown (on the left). Scale bar 300 µm

Fascin was positive in 26/30 cases with a cytoplasmic staining pattern, however, 7/26 were positive only at the invasion sites. In general, the staining intensity of Fascin was more pronounced at the invasion front and at the vascular invasion site as compared to the tumor center (Figure 26). All carcinomas positive for vimentin (9/30) were also Fascin-positive, although with a lesser intensity.

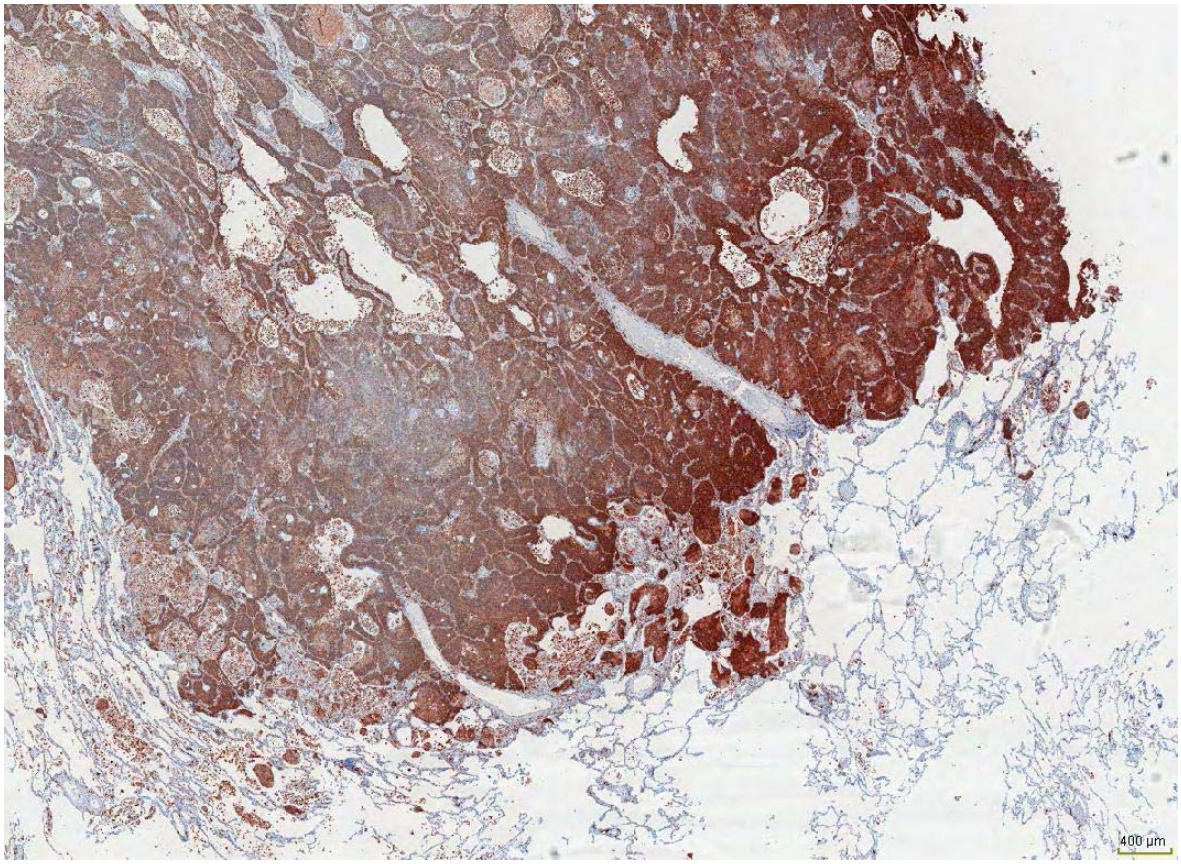

Figure 26: IHC Fascin with cytoplasmic staining pattern. The tumor center (top/left) is less intensely stained than the invasion front (middle/right). For spatial orientation, non-tumorous lung tissue is shown (bottom/right). Scale bar 400 µm

pERK1/2 was positive in 10/30 cases at the tumor center and in 16/30 cases at the invasion sites (Figure 27 and Figure 28). The staining pattern was predominantly cytoplasmic, but occasionally also nuclear. In 1/30 case, positivity was confined to the pleural invasion site.

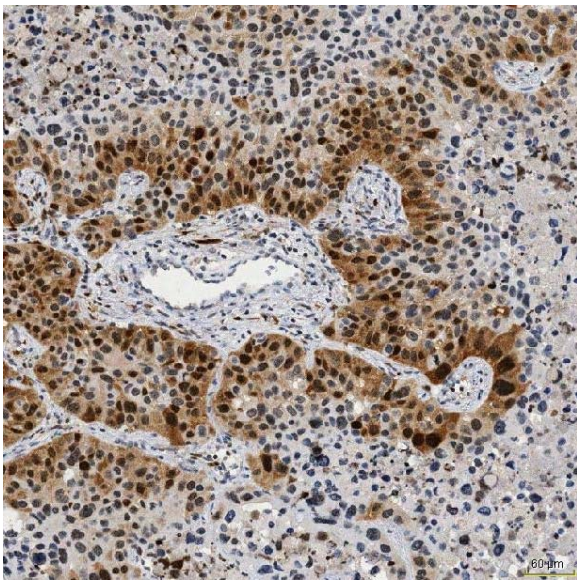

Figure 27: IHC pERK with cytoplasmic and nuclear staining pattern. The pERK-positive tumor cells (invasion front) are assembled around the blood vessel in the middle, whereas the pERK-negative tumor cells are located at the edge of the figure. Apparently, the tumor cells are about to infiltrate the blood vessel wall. Scale bar 60 µm

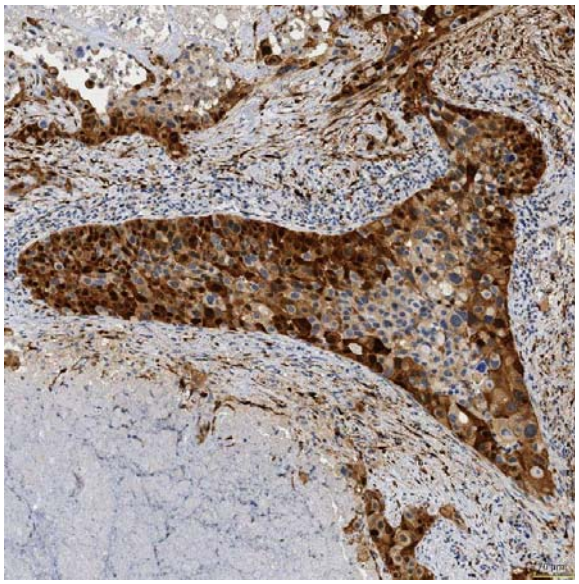

Figure 28: IHC pERK of the same case (different region) as in Figure 27 with cytoplasmic and, here to a lesser extent, nuclear staining pattern. The shown tumor complex is located within a blood vessel (vascular invasion site). Interestingly, the tumor cells at the center of this complex are less intensely stained than the ones along the edge (near the endothelium). Scale bar 70 µm

Connexin43 was positive in 20/30 cases with a cytoplasmic and membranous staining pattern. The positive tumor cells were mostly scattered over the tumor center and the invasion sites. At the latter, the scattered tumor cells were more numerous. However, in a few cases Connexin43-positivity was exceptionally strong (Figure 29 and Figure 30). CXCR1, CXCR2, and CXCR4 were expressed in 30/30, 11/30, and 9/30 cases, respectively. The staining patterns also differed between CXCR1 (cytoplasmic), CXCR2 (nuclear, cytoplasmic), and CXCR4 (cytoplasmic, membranous). All three markers were usually expressed focally without any differences in the number of positive cases between tumor center and invasion sites. However, CXCR2 was always less intensely stained at the invasion front. In all cases (30/30), a high CXCR2 staining intensity was prominent in macrophages.

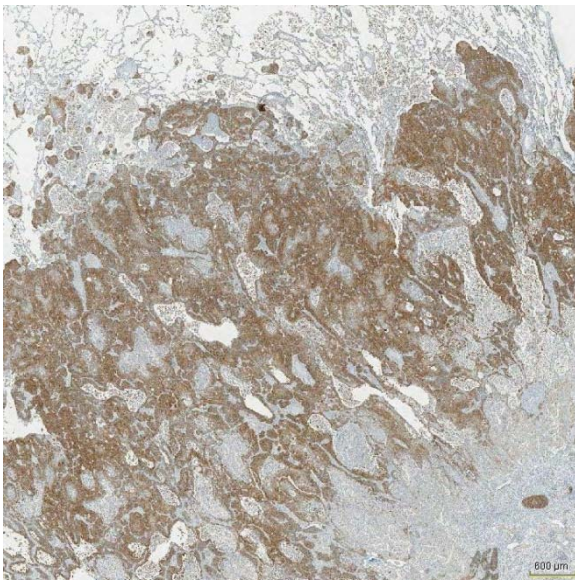

Figure 29: IHC Connexin43. The tumor tissue shows a strong and evenly distributed Connexin43-staining. The unstained regions on top and on the bottom right are non-tumorous tissue. Scale bar 600 µm

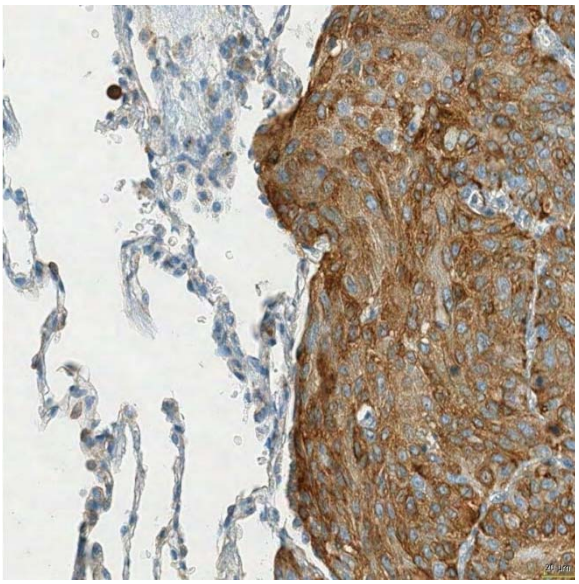

Figure 30: IHC Connexin43 of the same case as in Figure 29. The invasion front of the tumor (on the right) shows a strong Connexin43-positivity with a cytoplasmic and membranous staining pattern. For spatial orientation, non-tumorous lung tissue is shown (on the left). Scale bar 20 µm

PLCγ showed cytoplasmic positivity in 22/30 cases with stromal and pleural invasion. The tumor center was PLCγ-negative in all cases (Figure 31). Tumor cell complexes within the blood vessel walls or lumina also expressed PLCγ. RhoA was positive in 27/30 cases with a cytoplasmic staining pattern, both at the tumor center and at the invasion front/ vascular invasion site. However, the invasive sites were less intensely stained in comparison to the tumor center. CdC42 was focally positive at the invasion sites in 5/30 cases, only 2/30 were randomly positive in the tumor center. The staining pattern of CdC42 was cytoplasmic and membranous.

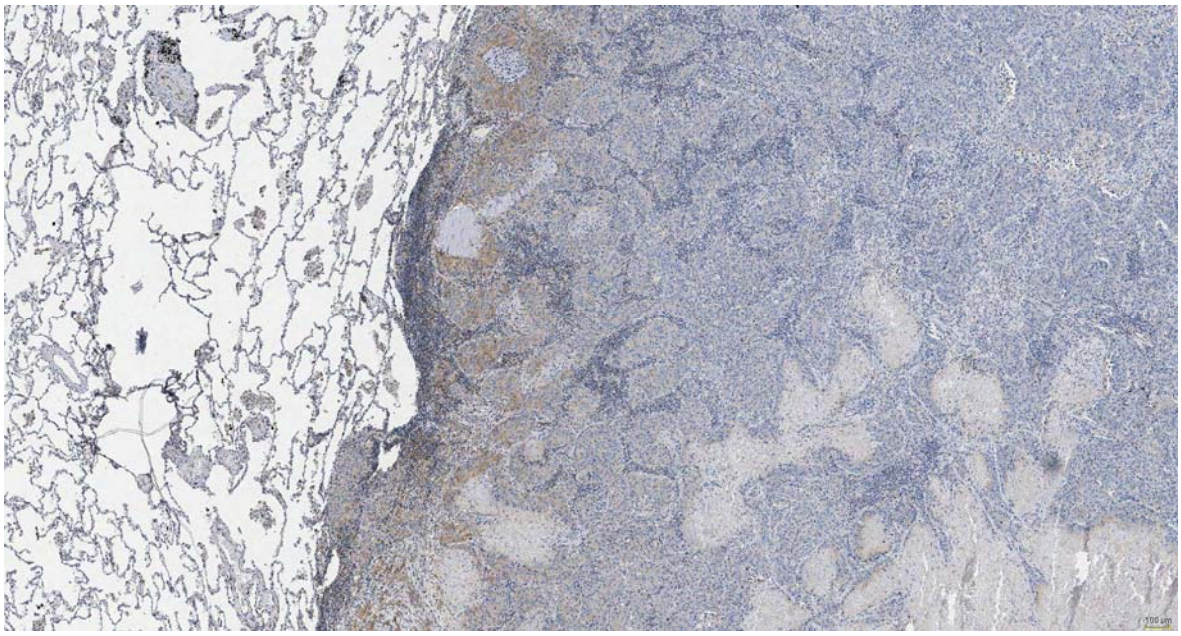

Figure 31: IHC PLCγ with cytoplasmic staining pattern. The invasion front (in the middle) is PLCγ-positive, wheras the tumor center (on the right) is PLCγ-negative. For spatial orientation, non-tumorous lung tissue is shown (on the left). Scale bar 100 µm

Focal adhesion kinase (FAK) was focally positive in 15/30 carcinomas (cytoplasmic staining pattern), with more intense staining in tumor centers. Integrin-linked kinase (ILK) was positive in 18/30 cases and showed a nuclear and cytoplasmic staining pattern. In 8/18 cases, ILK-positivity was confined to mitotic cells. The vascular invasion site was always negative for ILK (0/30). pSRC showed nuclear positivity in 6/30 tumors. In 4/6 tumors, exclusively mitotic cells were stained, 2/6 tumors were randomly nuclear positive. SARI was negative in all cases. SMARCA4, in contrast, was positive in all cases (nuclear staining pattern) without any staining differences between tumor center and invasion sites. YAP1 was positive in 29/30 cases with the invasion site always less intensely stained. In 8/29 cases, YAP1-staining was exclusively cytoplasmic, whereas in 21/29 cases, the staining was both cytoplasmic and nuclear. ZFPL1 was positive in 8/30 carcinomas. In 7/8 ZFPL1-positive carcinomas, only few predominantly keratinized SCC cells were stained. Only 1/8 case was diffusely positive. In general, the expression of ZFPL1 was confined to the tumor center in all positive cases (8/8) and showed a nuclear and cytoplasmic staining pattern.

4.2 Validation set

In the validation set we evaluated the 9 markers E-cadherin, N-cadherin, pERK, Twist, Vimentin, Mad, Tks5, PLCγ and Connexin43. Either the staining extent (percentage) or the staining intensity (score) was assessed. Positivity was defined by a staining extent of at least 1% or by a staining intensity score of at least 1 (see also Material/Methods chapter). In the following, the results of these three parameters (positivity, extent, and intensity) will be presented. Due to the qualitative approach in the study set and the spatial limitations of TMAs, the only parameter that could be compared between the study set and the validation set is the number of positive cases. The other parameters (extent or intensity) could only be compared between different subpopulations within the validation set.

The markers with the highest number of positive cases in the validation set were N-cad (99.6%), E-cad (98.1%), and Mad (81,5%). The markers with the lowest number of positive cases were Vimentin (32.8%), Tks5 (48.8%), and PLCγ (55.6%). By comparing the validation set with the study set in terms of positively stained cases, some marker-specific differences were identified (Figure 32). Specifically, pERK was positive in more cases of the validation set (67.2%) than in the study set (33.3% and 53.3%). Conversely, Twist, Tks5, and PLCγ positivity was more abundant in the study set. E-Cad, N-Cad, Mad, and Con43 showed no considerable difference in positive cases between validation set and study set.

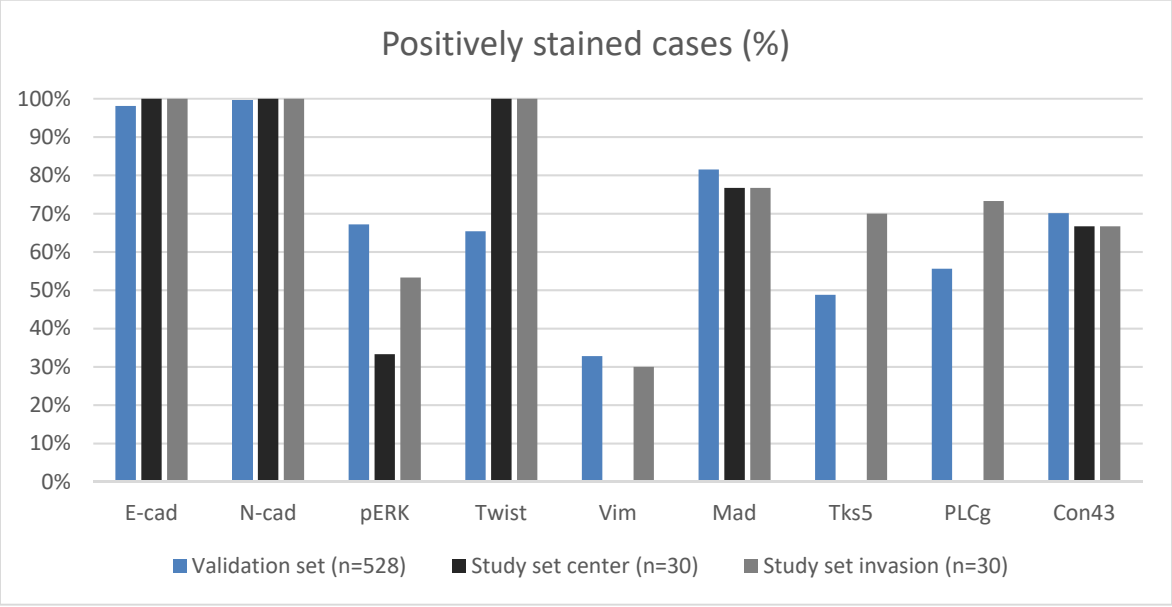

Figure 32: Percentages of positive cases in the validation set in comparison to the study set

Comparing ACs, SCCs, and LCs within the validation set, there were also marker-specific differences in expression (Figure 33). In LCs, there were less cadherin-expressing tumor cells (both E-cad and N-cad) than in the other histological subtypes. In contrast, pERK was most often expressed in LCs. Twist was most often positive in SCCs and LCs (83.8% and 78.4%, respectively), compared against ACs with only 50.7% twist-positive tumor cells. Vimentin was least often expressed in SCCs (only 15.2%). In contrast, both Tks5 and Con43 were mostly positive in SCCs (73.2% and 94.2%, respectively).

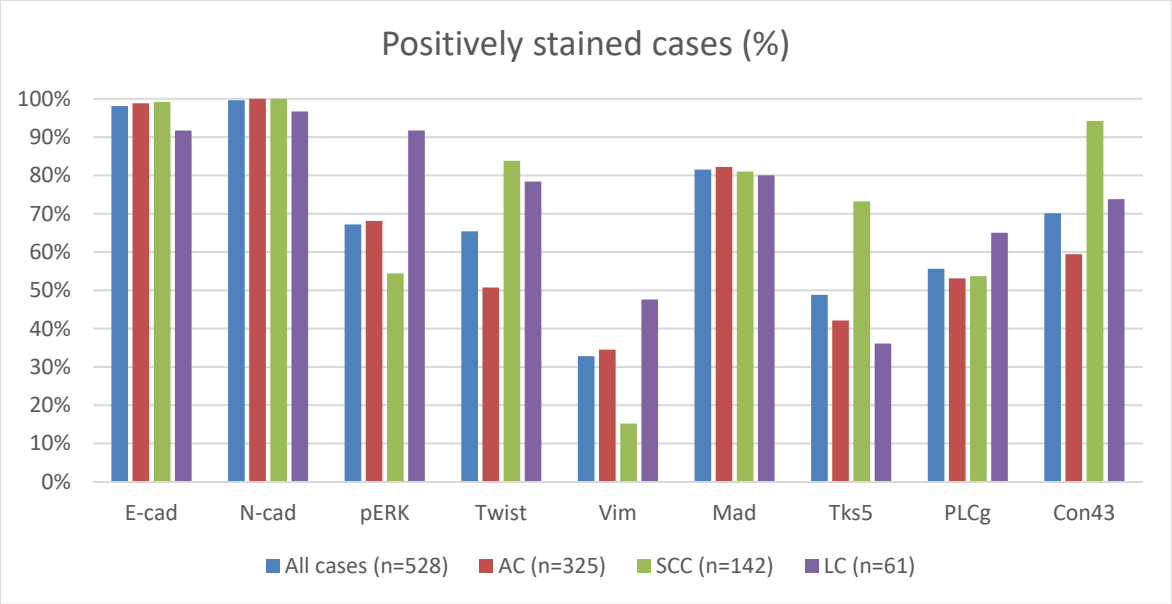

Figure 33: Percentages of positive cases in the validation set in total, as well as separately in AC, SCC, and LC

Due to differences in the spatial distribution of the respective markers, the TMA-cores represent different amounts of positively stained tumor cells. Figure 34 and Figure 35 illustrate these differences by comparing the missing TMA-cores between the Twist- and the Vimentin-staining of the same donor block. Figure 36 and Figure 37 show the resulting punched TMA-cores with different amounts of Twist- and Vimentin-positivity.

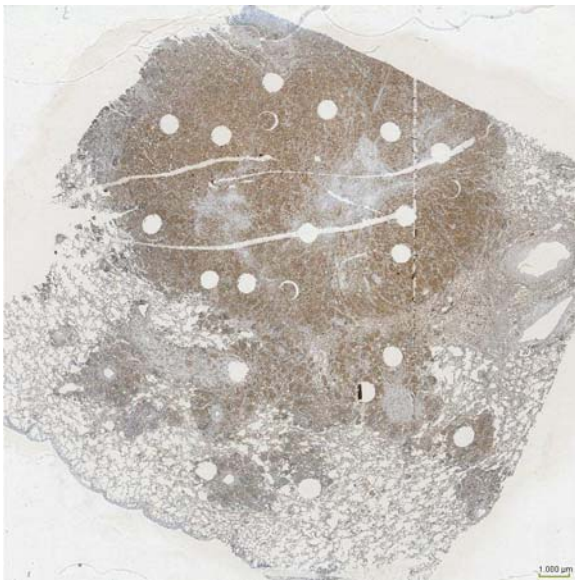

Figure 34: IHC Twist of a TMA donor block section. The round holes throughout the specimen represent the missing cores after TMA preparation. They are located almost exclusively within Twist-positive tumor tissue (brown area). Scale bar 1000µm

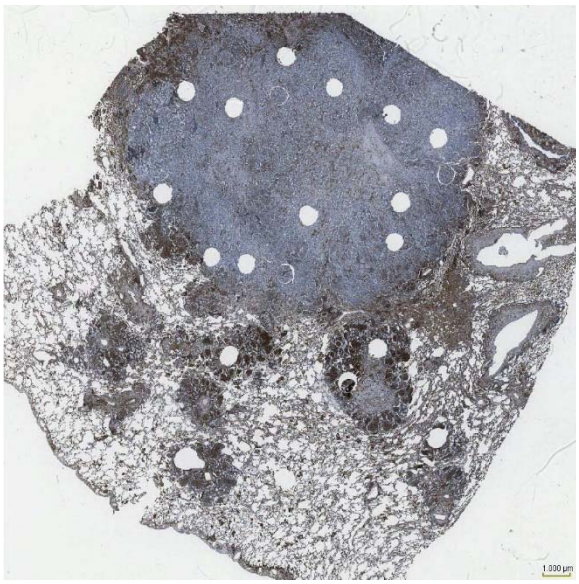

Figure 35: IHC Vimentin of the same TMA donor block as in Figure 34. The missing TMA-cores are located mostly within Vimentin-negative tumor tissue (blue area). Scale bar 1000 µm.

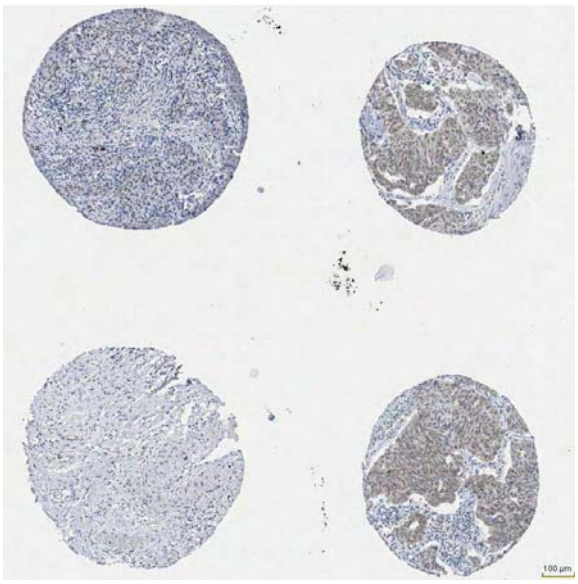

Figure 36: IHC Twist of a (partial) TMA recipient block section with four representative cores. The upper left core shows partially positive tumor tissue with a nuclear staining pattern. Both the upper and lower right core show completely positive tumor tissue with a both nuclear and cytoplasmic staining pattern. The lower left core shows non-tumorous lung tissue. In all four cases, the stroma is completely negative. Scale bar 100µm.

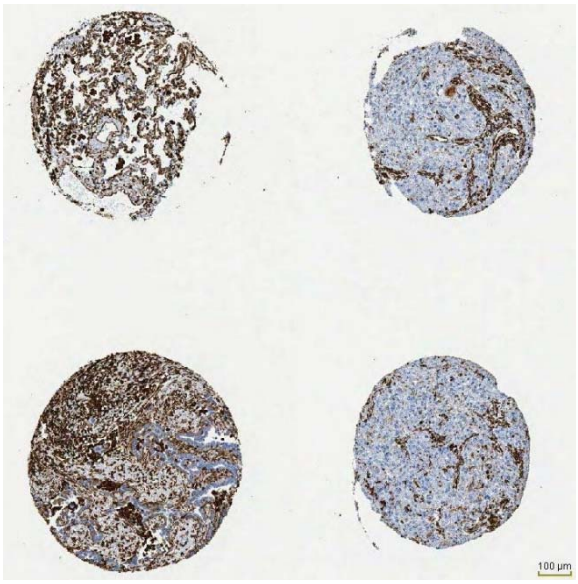

Figure 37: IHC Vimentin of a (partial) TMA recipient block section with four representative cores. The upper left core shows non-tumorous lung tissue. Both the upper and lower right core contain only Vimentin-negative tumor tissue with positivity confined to the stroma. The lower left core shows partially positive tumor tissue with a cytoplasmic staining pattern, whereas the stroma is again completely positive. Scale bar 100µm.

The three markers E-cad, N-cad, and pERK were evaluated in terms of their staining intensity, regardless of the number of positive tumor cells (Figure 38). In general, pERK was the least intensely stained marker (mean intensity 0.71), as opposed to E-cad and N-cad (1.10 and 1.13, respectively). E-cad was the most intensely stained marker in SCCs (1.23). For N-cad, there were no significant differences between histological subtypes. pERK was most intensely stained in LCs (1.03) and least intensely in SCCs (0.47).

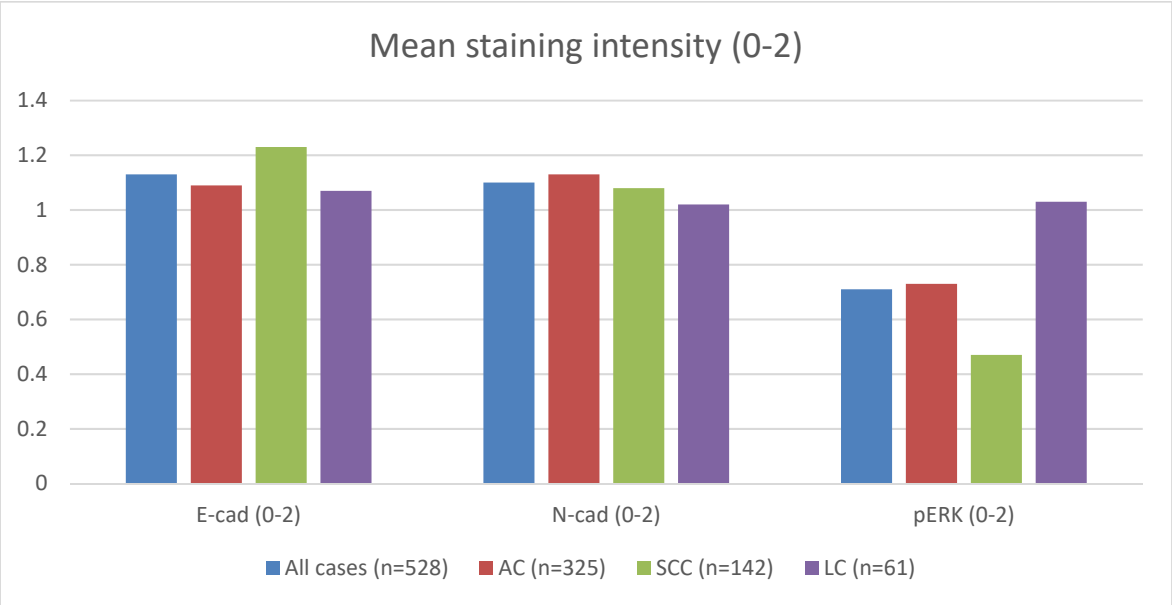

Figure 38: Mean staining intensity (score 0-2) for E-cad, N-cad, and pERK

The markers Twist, Vimentin, Mad, Tks5, PLCγ, and Connexin43 were evaluated in terms of their staining extent (Figure 39). In general, the most widely expressed markers were Mad (mean extent 33.5%), Connexin43 (29.0%), and Twist (24.0%). The least widely expressed markers were Tks5 (7.8%), Vimentin (8.9%), and PLCγ (14.1%). Twist showed some differences between histological subtypes: 40.6% in SCCs versus 17.2% in ACs. Vimentin had the most widely expressed positivity in LCs (19.9%). Tks5 and Connexin43 were both most widely expressed in SCCs (16.5% and 53.1%, respectively). Both Mad and PLCγ showed no significant differences between histological subtypes.

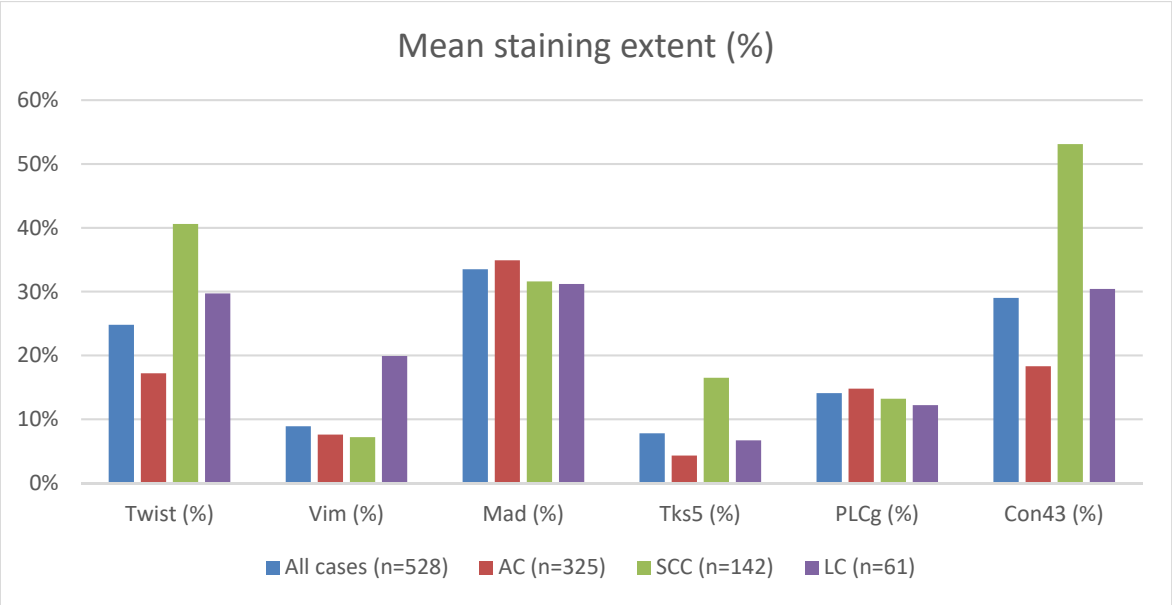

Figure 39: Mean staining extent (%) for Twist, Vim, Mad, Tks5, PLCγ, and Con43

5 DISCUSSION

In this study, we evaluated the role of the EMT and other migration-associated molecules in NSCLC invasion. In the following, all studied markers with interesting results will be discussed, comprising both EMT-associated markers and molecules connected to migration and metastasis in general.

Regarding EMT, Twist was the only EMT transcription factor which was expressed in all cases. However, as TGFß was negative in all our cases, Twist was presumably not induced by TGFß, which is in contrast to previous reports in the literature (137). Therefore, Twist must have been induced by other factors. One possibility is hypoxia: It has been reported that intratumoral hypoxia leads to upregulation of twist via HIF-1alpha and that this signaling pathway promotes metastasis (138). In this context it is interesting to note that also in mouse models of lung adenocarcinomas, the invasion of tumor cells started exclusively in areas of hypoxia (139). Snail was expressed in less than half of our cases and only in scattered single cells. Hence, in our study we could not confirm the role of Twist as an inducer of Snail, as described in the literature (140). The fact that ZEB1 and Slug were both negative in almost all cases, provides further evidence for the lack of classical EMT in NSCLC bulk migration.

E-cadherin was downregulated at the invasion front and at the vascular invasion site, but its expression was never completely lost. Conversely, the staining of N-Cadherin was more intense at the invasion sites. However, N-cadherin was also expressed in all cases. The coexpression of both cadherins provides evidence for a cell phenotype that is not exclusively mesenchymal or epithelial, but rather a state in between. This conclusion is supported by recent in-vitro findings, which have shown that a hybrid epithelial/mesenchymal state is a stable cell phenotype (141). In our cases, vimentin positive tumor cells at the invasion sites also co-expressed epithelial markers. This is in line with the assumption that cells within migrating cell complexes can be subdivided into leader cells (at the front) and follower cells (at the rear). This concept supports the idea that only cells at the invasion front must obtain some mesenchymal features, in order to pave the way for the following cell bulk (142). Based on this concept, the vimentin positive tumor cells in our study set were probably the leader cells. However, vimentin was positive in only a third of our cases. Other mechanisms

must therefore also be involved in this process. Interestingly, it has been recently shown that cancer-associated fibroblasts (CAFs) mechanically interact with cancer cells via N-cadherin (at the fibroblast membrane) and E-cadherin (at the cancer cell membrane). This heterotypic interaction exerts a physical force on cancer cells and enables migration (143). Consequently, fibroblasts might act as leader cells in the vimentin negative cases of our study set. However, the exact role of CAFs in tumor cell migration is still quite controversial, and other mechanisms that pave the way for the follower cells are also possible.

In conclusion, our findings regarding EMT markers provide evidence that an EMT is not indispensable for tumor cell migration in NSCLC. This is in line with two very recent and pivotal studies which have shown that cancer cells do not require EMT to accomplish metastasis (144,145).

In addition to molecules related to EMT, we also studied factors related to cell migration in general. Among the tested molecules which have been described as being important for wing border cell migration in drosophila (101), Rack1 and Sax were negative in all our cases. In contrast, Mad was expressed in most, and Brk in half of our cases in the study set. The number of Mad-positive tumor cells was similar in the study set and in the validation set. These findings indicate that some of the molecules found in drosophila might also have a role in human bulk tumor cell migration. However, in drosophila the expression of these molecules was accompanied by an upregulation of TGFß (101), whereas in our cases this association could not be observed.

An interesting finding in our study was that three examined molecules (Rab40B, Tks5, Fascin), which have been described to be associated with invadopodia formation or stabilization (105), were clearly upregulated at the invasion sites. In half of the study set cases, Rab40B and Tks5 were even coexpressed. Hence, it is very likely that invadopodia play an important role in bulk tumor cell migration. The markers pERK and PLCγ were also significantly upregulated at the invasion front and at the vascular invasion site, thus providing evidence for their role in cell migration. With these findings we could also confirm previous reports regarding the activation of ERK1/2 in NSCLC and its association with advanced tumors (111). As PLCγ has been described to be related to both blood vessel development (112) and cancer cell invasion (114), the upregulation of PLCγ in our study might be a result of angiogenesis during invasion.

Within the studied RhoGTPases, RhoA was more intensely stained at the tumor center, whereas CdC42 was positive mostly at the invasion sites. Hence, the above described feature of E-cadherin to downregulate RhoGTPases (96) could only be confirmed for CdC42 at the tumor center. The downregulation of RhoA at the invasion sites was therefore probably induced by another factor.

As Connexin43 was expressed in two thirds of our cases, it might have contributed to the downregulation of several EMT markers. This finding is in accordance with a recent report, claiming that Connexin43 overexpression reverses EMT in NSCLC (120). The previously described involvement of CXCR1 in EMT (124) could not be validated in our study, since CXCR1 was expressed in all our cases despite the widespread lack of EMT-phenotypes. Even though CXCR2 was only expressed in one third of our cases in the tumor cells, the staining intensity in macrophages was very high in all 30 cases. Thus, the role of CXCR2 in inflammation-driven tumorigenesis (126) could possibly be mediated by tumor-infiltrating macrophages. CXCR4 was also expressed in about one third of our cases. Although this is in line with the general frequency of brain metastasis in NSCLC (146), further studies are needed to validate the correlation of CXCR4 with brain-specific metastasis (129). This could be done for example by comparing the expression of CXCR4 between the primary tumor and the matched metastatic brain lesions in the same patients.

SMARCA4 was positive in all our cases, thus contradicting a study which states that SMARCA4 loss is associated with a more aggressive tumor phenotype (131), since the vascular invasion in all our cases can be seen as a sign of aggressiveness. Also the correlation of SMARCA4 loss with a differentiated histological phenotype (132) is in conflict with our data, because all tumors of our study set were at least moderately differentiated and still retained SMARCA4 expression. In many of our ILK-positive cases, the staining was exclusively positive for mitotic cells. This is in accordance with a report claiming that ILK is localized in centrosomes and that it regulates the organization of the mitotic spindle (147).

The nine markers that were additionally evaluated in the validation set (E-cadherin, N-cadherin, pERK, Twist, Vimentin, Mad, Tks5, PLCγ and Connexin43) showed mostly a similar number of positive cases when compared to the study set. However, for some markers the differences were more distinct than for others (Figure 32). One explanation for these discrepancies are the varying spatial distributions among the different markers,

including the tumor center and the tumor margins (Figures 34-37). As a consequence, the punched TMA-cores contained different amounts of positive tumor cells, especially in markers with a pronounced staining at the invasion front (Vimentin, Tks5, and PLCγ).

6 CONCLUSION

By investigating a variety of molecules associated with cell migration, we could confirm many findings previously described in the literature. However, there were also some novel findings in our study cohort: On the one hand, we could identify several new molecules being involved in NSCLC invasion, which never had been linked to metastasis before. On the other hand, our findings provide evidence that some well-known migratory signaling pathways are also present in NSCLC bulk migration, but are regulated maybe in a slightly different way than previously reported. This discrepancy can most likely be explained by the fact that many of the above-mentioned studies have been done in a setting of single cell migration, while the tumor cells in our cases moved predominantly via collective cell migration.

In general, the migration capacity of tumor cell bulks is acknowledged beyond controversy in the literature. However, to what extent these tumor cell clusters contribute to metastasis is still controversial. In a recent study it could be demonstrated that the occurrence of circulating tumor cell clusters is associated with a worse prognosis as compared with the occurrence of single circulating tumor cells (148). This study along with other findings (149) provide evidence that tumor cell clusters are very efficient in disseminating and seeding of metastatic colonies.

Therefore, it is of prime clinical importance to better understand this movement of cell bulks in cancer. Our study provides at least some new aspects to this still insufficient understanding: 1) There are remarkable differences in the expression of involved molecules and in the regulation of these molecules between single cell and collective cell invasion; 2) NSCLC tumor cell bulks predominantly show a cell phenotype that has both epithelial and mesenchymal characteristics, which is probably the result of a partial EMT rather than EMT in its classical binary (epithelial or mesenchymal) form. However, to gain further mechanistic insight, future studies must validate and specify these findings in an experimental setting. Finally, the clinical significance of our findings must be elucidated by correlating obtained results to patient data.

REFERENCES

1. GLOBOCAN_Lung [Internet]. [cited 2017 Aug 8]. Available from: http://globocan.iarc.fr/Pages/fact_sheets_cancer.aspx
2. Brambilla E, Travis W. Lung cancer. In: Stewart B, Wild C, editors. World Cancer Report. Lyon: World Health Organization; 2014.
3. Torre LA, Bray F, Siegel RL, Ferlay J. Global Cancer Statistics , 2012. CAA cancer J Clin. 2015;
4. Malvezzi M, Carioli G, Bertuccio P, Boffetta P, Levi F, La Vecchia C, et al. European cancer mortality predictions for the year 2017, with focus on lung cancer. Ann Oncol. 2017 May 1;28(5):1117–23.
5. Ferlay J, Steliarova-Foucher E, Lortet-Tieulent J, Rosso S, Coebergh JWW, Comber H, et al. Cancer incidence and mortality patterns in Europe: Estimates for 40 countries in 2012. Eur J Cancer. 2013 Apr;49(6):1374–403.
6. Statistik Austria_Krebserkrankungen_Luftröhre, Bronchien, Lunge [Internet]. [cited 2017 Aug 8]. Available from: http://www.statistik.at/web_de/statistiken/menschen_und_gesellschaft/gesundheit/krebserkrankungen/luftroehre_bronchien_lunge/index.html
7. Fielding JE. Smoking: Health Effects and Control. N Engl J Med. 1985 Aug 22;313(8):491–8.
8. Ezzati M, Lopez AD. Estimates of global mortality attributable to smoking in 2000. Lancet. 2003 Sep 13;362(9387):847–52.
9. Doll R, Peto R, Boreham J, Sutherland I. Mortality in relation to smoking: 50 years' observations on male British doctors. BMJ. 2004 Jun 26;328(7455):1519.
10. Hubbard R, Venn A, Lewis S, Britton J. Lung Cancer and Cryptogenic Fibrosing Alveolitis. Am J Respir Crit Care Med. 2000 Jan;161(1):5–8.
11. Alberg AJ, Brock M V., Ford JG, Samet JM, Spivack SD. Epidemiology of lung cancer: Diagnosis and management of lung cancer, 3rd ed: American College of Chest Physicians evidence-based clinical practice guidelines. Chest. 2013 May;143(5 Suppl):e1S–e29S.
12. Saracci R. The interactions of tobacco smoking and other agents in cancer etiology. Epidemiol Rev. 1987;9:175–93.
13. Travis, W.D., Brambilla, E., Burke, A.P., Marx, A., Nicholson AG. WHO

Classification of Tumours of the Lung, Pleura, Thymus, and Heart. Lyon: IARC Press; 2015.

14. Tazelaar HD. Pathology of lung malignancies [Internet]. [cited 2017 Aug 21]. Available from: https://www.uptodate.com/contents/pathology-of-lung-malignancies
15. Travis WD, Brambilla E, Nicholson AG, Yatabe Y, Austin JHM, Beasley MB, et al. The 2015 World Health Organization Classification of Lung Tumors: Impact of Genetic, Clinical and Radiologic Advances Since the 2004 Classification. J Thorac Oncol. 2015 Sep 1;10(9):1243–60.
16. Popper H. Pathology of Lung Disease. Heidelberg: Springer; 2017.
17. Janssen-Heijnen ML, Coebergh JW, Klinkhamer PJ, Schipper RM, Splinter TA, Mooi WJ. Is there a common etiology for the rising incidence of and decreasing survival with adenocarcinoma of the lung? Epidemiology. 2001 Mar;12(2):256–8.
18. Travis WD, Brambilla E, Noguchi M, Nicholson AG, Geisinger KR, Yatabe Y, et al. International association for the study of lung cancer/american thoracic society/european respiratory society international multidisciplinary classification of lung adenocarcinoma. J Thorac Oncol. 2011 Feb;6(2):244–85.
19. Kadota K, Yeh Y-C, Sima CS, Rusch VW, Moreira AL, Adusumilli PS, et al. The cribriform pattern identifies a subset of acinar predominant tumors with poor prognosis in patients with stage I lung adenocarcinoma: a conceptual proposal to classify cribriform predominant tumors as a distinct histologic subtype. Mod Pathol. 2014 May 1;27(5):690–700.
20. Kadota K, Nitadori J, Rekhtman N, Jones DR, Adusumilli PS, Travis WD. Reevaluation and Reclassification of Resected Lung Carcinomas Originally Diagnosed as Squamous Cell Carcinoma Using Immunohistochemical Analysis. Am J Surg Pathol. 2015 Sep;39(9):1170–80.
21. Filosso PL, Ruffini E, Asioli S, Giobbe R, Macri L, Bruna MC, et al. Adenosquamous lung carcinomas: A histologic subtype with poor prognosis. Lung Cancer. 2011 Oct;74(1):25–9.
22. Yendamuri S, Caty L, Pine M, Adem S, Bogner P, Miller A, et al. Outcomes of sarcomatoid carcinoma of the lung: A Surveillance, Epidemiology, and End Results database analysis. Surgery. 2012 Sep;152(3):397–402.
23. Caplin ME, Baudin E, Ferolla P, Filosso P, Garcia-Yuste M, Lim E, et al. Pulmonary neuroendocrine (carcinoid) tumors: European Neuroendocrine Tumor Society expert consensus and recommendations for best practice for typical and atypical pulmonary

carcinoids. Ann Oncol. 2015 Aug;26(8):1604–20.

24. Fernandez-Cuesta L, Peifer M, Lu X, Sun R, Ozretić L, Seidel D, et al. Frequent mutations in chromatin-remodelling genes in pulmonary carcinoids. Nat Commun. 2014 Mar 27;5:3518.
25. Vogelstein B, Kinzler KW. The multistep nature of cancer. Trends Genet. 1993 Apr;9(4):138–41.
26. Wistuba II, Behrens C, Milchgrub S, Bryant D, Hung J, Minna JD, et al. Sequential molecular abnormalities are involved in the multistage development of squamous cell lung carcinoma. Oncogene. 1999 Feb 2;18(3):643–50.
27. Yatabe Y, Borczuk AC, Powell CA. Do all lung adenocarcinomas follow a stepwise progression? Lung Cancer. 2011 Oct;74(1):7–11.
28. Kadara H, Wistuba II. Field Cancerization in Non–Small Cell Lung Cancer. Proc Am Thorac Soc. 2012 May;9(2):38–42.
29. Wistuba II, Gazdar AF. Lung cancer preneoplasia. Annu Rev Pathol Mech Dis. 2006 Feb;1(1):331–48.
30. Imielinski M, Berger AH, Hammerman PS, Hernandez B, Pugh TJ, Hodis E, et al. Mapping the hallmarks of lung adenocarcinoma with massively parallel sequencing. Cell. 2012 Sep 14;150(6):1107–20.
31. Rodenhuis S, Slebos RJ, Boot AJ, Evers SG, Mooi WJ, Wagenaar SS, et al. Incidence and possible clinical significance of K-ras oncogene activation in adenocarcinoma of the human lung. Cancer Res. 1988 Oct 15;48(20):5738–41.
32. Mounawar M, Mukeria A, Le Calvez F, Hung RJ, Renard H, Cortot A, et al. Patterns of EGFR, HER2, TP53, and KRAS Mutations of p14arf Expression in Non-Small Cell Lung Cancers in Relation to Smoking History. Cancer Res. 2007 Jun 15;67(12):5667–72.
33. Kitamura H, Kameda Y, Ito T, Hayashi H. Atypical adenomatous hyperplasia of the lung. Implications for the pathogenesis of peripheral lung adenocarcinoma. Am J Clin Pathol. 1999 May;111(5):610–22.
34. Westra WH, Baas IO, Hruban RH, Askin FB, Wilson K, Offerhaus GJ, et al. K-ras oncogene activation in atypical alveolar hyperplasias of the human lung. Cancer Res. 1996 May 1;56(9):2224–8.
35. Yatabe Y, Mitsudomi T, Takahashi T. TTF-1 expression in pulmonary adenocarcinomas. Am J Surg Pathol. 2002 Jun;26(6):767–73.
36. Kwei KA, Kim YH, Girard L, Kao J, Pacyna-Gengelbach M, Salari K, et al. Genomic

profiling identifies TITF1 as a lineage-specific oncogene amplified in lung cancer. Oncogene. 2008 Jun 5;27(25):3635–40.

37. Rock JR, Randell SH, Hogan BLM. Airway basal stem cells: a perspective on their roles in epithelial homeostasis and remodeling. Dis Model Mech. 2010 Sep 1;3(9–10):545–56.

38. Belinsky SA, Nikula KJ, Palmisano WA, Michels R, Saccomanno G, Gabrielson E, et al. Aberrant methylation of p16(INK4a) is an early event in lung cancer and a potential biomarker for early diagnosis. Proc Natl Acad Sci U S A. 1998 Sep 29;95(20):11891–6.

39. Merrick DT, Haney J, Petrunich S, Sugita M, Miller YE, Keith RL, et al. Overexpression of vascular endothelial growth factor and its receptors in bronchial dypslasia demonstrated by quantitative RT-PCR analysis. Lung Cancer. 2005 Apr;48(1):31–45.

40. Bass AJ, Watanabe H, Mermel CH, Yu S, Perner S, Verhaak RG, et al. SOX2 is an amplified lineage-survival oncogene in lung and esophageal squamous cell carcinomas. Nat Genet. 2009 Nov 4;41(11):1238–42.

41. Yuan P, Kadara H, Behrens C, Tang X, Woods D, Solis LM, et al. Sex Determining Region Y-Box 2 (SOX2) Is a Potential Cell-Lineage Gene Highly Expressed in the Pathogenesis of Squamous Cell Carcinomas of the Lung. Lau ATY, editor. PLoS One. 2010 Feb 9;5(2):e9112.

42. McCaughan F, Pole JCM, Bankier AT, Konfortov BA, Carroll B, Falzon M, et al. Progressive 3q amplification consistently targets SOX2 in preinvasive squamous lung cancer. Am J Respir Crit Care Med. 2010 Jul 1;182(1):83–91.

43. Wistuba II, Behrens C, Virmani AK, Mele G, Milchgrub S, Girard L, et al. High resolution chromosome 3p allelotyping of human lung cancer and preneoplastic/preinvasive bronchial epithelium reveals multiple, discontinuous sites of 3p allele loss and three regions of frequent breakpoints. Cancer Res. 2000 Apr 1;60(7):1949–60.

44. Watkins DN, Berman DM, Burkholder SG, Wang B, Beachy PA, Baylin SB. Hedgehog signalling within airway epithelial progenitors and in small-cell lung cancer. Nature. 2003 Mar 20;422(6929):313–7.

45. Peifer M, Fernández-Cuesta L, Sos ML, George J, Seidel D, Kasper LH, et al. Integrative genome analyses identify key somatic driver mutations of small-cell lung cancer. Nat Genet. 2012 Sep 2;44(10):1104–10.

46. Powell CA, et al. Molecular testing for treatment selection in lung cancer. In: Travis WD, editor. WHO Classification of Tumours of the Lung, Pleura, Thymus and Heart. 4th ed. Lyon: International Agency for Research on Cancer; 2015. p. 22–5.
47. Kadara H, Scheet P, Wistuba II, Spira AE. Early Events in the Molecular Pathogenesis of Lung Cancer. Cancer Prev Res. 2016;9(7).
48. Dooms C. Diagnosing lung cancer. In: Stahel RA, Peters S, Garassino M, editors. Thoracic Tumours - Essentials for Cinicians. Lugano: ESMO Press; 2014. p. 14–9.
49. Braun J, Renz-Polster H. Neoplastische Lungenerkrankungen. In: Renz-Polster H, Krautzig S, editors. Basislehrbuch Innere Medizin. 5th ed. München: Elsevier; 2013. p. 452–6.
50. MacMahon H, Austin JHM, Gamsu G, Herold CJ, Jett JR, Naidich DP, et al. Guidelines for Management of Small Pulmonary Nodules Detected on CT Scans: A Statement from the Fleischner Society. Radiology. 2005 Nov;237(2):395–400.
51. Hoda M, Klepetko W. Principles of surgery of non-small cell lung cancer. In: Stahel RA, Peters S, Garassino M, editors. Thoracic Tumours - Essentials for Cinicians. Lugano: ESMO Press; 2014. p. 26–37.
52. Senan S. Principles of radiotherapy of thoracic tumours. In: Stahel R, Peters S, Garassino M, editors. Thoracic Tumours - Essentials for Cinicians. Lugano: ESMO Press; 2014. p. 32–7.
53. Schiller JH, Harrington D, Belani CP, Langer C, Sandler A, Krook J, et al. Comparison of Four Chemotherapy Regimens for Advanced Non–Small-Cell Lung Cancer. N Engl J Med. 2002 Jan 10;346(2):92–8.
54. Novello S, Barlesi F, Califano R, Cufer T, Ekman S, Levra MG, et al. Metastatic non-small-cell lung cancer: ESMO Clinical Practice Guidelines for diagnosis, treatment and follow-up†. Ann Oncol. 2016 Sep;27(suppl_5):v1–27.
55. Sullivan I, Planchard D. ALK inhibitors in non-small cell lung cancer: the latest evidence and developments. Ther Adv Med Oncol. 2016 Jan;8(1):32–47.
56. European Medicines Agency - Keytruda [Internet]. [cited 2017 Aug 31]. Available from: http://www.ema.europa.eu/ema/index.jsp?curl=pages/medicines/human/medicines/003820/human_med_001886.jsp&mid=WC0b01ac058001d124
57. European Medicines Agency - Opdivo [Internet]. [cited 2017 Aug 31]. Available from: http://www.ema.europa.eu/ema/index.jsp?curl=pages/medicines/human/medicines/0

03985/human_med_001876.jsp&mid=WC0b01ac058001d124

58. Couzin-Frankel J. Cancer Immunotherapy. Science (80-). 2013 Dec 20;342(6165):1432–3.
59. Hanahan D, Weinberg RA. Hallmarks of Cancer: The Next Generation. Cell. 2011 Mar 4;144(5):646–74.
60. Thiery JP, Acloque H, Huang RYJ, Nieto MA. Epithelial-Mesenchymal Transitions in Development and Disease. Cell. 2009 Nov 25;139(5):871–90.
61. Hanahan D, Weinberg RA. The Hallmarks of Cancer. Cell. 2000 Jan;100(1):57–70.
62. Hüsemann Y, Geigl JB, Schubert F, Musiani P, Meyer M, Burghart E, et al. Systemic Spread Is an Early Step in Breast Cancer. Cancer Cell. 2008 Jan;13(1):58–68.
63. Clark AG, Vignjevic DM. Modes of cancer cell invasion and the role of the microenvironment. Curr Opin Cell Biol. 2015 Oct;36:13–22.
64. Brierley J, Gospodarowicz MK (Mary K., Wittekind C (Christian). TNM classification of malignant tumours. 8th ed. Hoboken: Wiley-Blackwell; 253 p.
65. Gay LJ, Felding-Habermann B. Contribution of platelets to tumour metastasis. Nat Rev Cancer. 2011 Feb;11(2):123–34.
66. Gasic GJ, Gasic TB, Stewart CC. Antimetastatic effects associated with platelet reduction. Proc Natl Acad Sci U S A. 1968 Sep;61(1):46–52.
67. Zhang X, Ran Y. Prognostic role of elevated platelet count in patients with lung cancer: a systematic review and meta-analysis. Int J Clin Exp Med. 2015;8(4):5379–87.
68. Palumbo JS, Talmage KE, Massari J V, La Jeunesse CM, Flick MJ, Kombrinck KW, et al. Platelets and fibrin(ogen) increase metastatic potential by impeding natural killer cell-mediated elimination of tumor cells. Blood. 2005 Jan 1;105(1):178–85.
69. Kopp H-G, Placke T, Salih HR. Platelet-Derived Transforming Growth Factor- Down-Regulates NKG2D Thereby Inhibiting Natural Killer Cell Antitumor Reactivity. Cancer Res. 2009 Oct 1;69(19):7775–83.
70. Labelle M, Begum S, Hynes RO. Direct Signaling between Platelets and Cancer Cells Induces an Epithelial-Mesenchymal-Like Transition and Promotes Metastasis. Cancer Cell. 2011 Nov 15;20(5):576–90.
71. Granot Z, Henke E, Comen EA, King TA, Norton L, Benezra R. Tumor Entrained Neutrophils Inhibit Seeding in the Premetastatic Lung. Cancer Cell. 2011 Sep 13;20(3):300–14.
72. Cools-Lartigue J, Spicer J, McDonald B, Gowing S, Chow S, Giannias B, et al.

Neutrophil extracellular traps sequester circulating tumor cells and promote metastasis. J Clin Invest. 2013 Aug 1;123(8):3446–58.

73. Spiegel A, Brooks MW, Houshyar S, Reinhardt F, Ardolino M, Fessler E, et al. Neutrophils Suppress Intraluminal NK Cell-Mediated Tumor Cell Clearance and Enhance Extravasation of Disseminated Carcinoma Cells. Cancer Discov. 2016 Jun 1;6(6):630–49.
74. Al-Mehdi AB, Tozawa K, Fisher AB, Shientag L, Lee A, Muschel RJ. Intravascular origin of metastasis from the proliferation of endothelium-attached tumor cells: a new model for metastasis. Nat Med. 2000 Jan;6(1):100–2.
75. Strilic B, Yang L, Albarrán-Juárez J, Wachsmuth L, Han K, Müller UC, et al. Tumour-cell-induced endothelial cell necroptosis via death receptor 6 promotes metastasis. Nature. 2016 Aug 3;536(7615):215–8.
76. Schumacher D, Strilic B, Sivaraj KK, Wettschureck N, Offermanns S. Platelet-Derived Nucleotides Promote Tumor-Cell Transendothelial Migration and Metastasis via P2Y2 Receptor. Cancer Cell. 2013 Jul 8;24(1):130–7.
77. Luzzi KJ, MacDonald IC, Schmidt EE, Kerkvliet N, Morris VL, Chambers AF, et al. Multistep Nature of Metastatic Inefficiency. Am J Pathol. 1998 Sep;153(3):865–73.
78. Giancotti FG. Mechanisms Governing Metastatic Dormancy and Reactivation. Cell. 2013 Nov 7;155(4):750–64.
79. Shibue T, Brooks MW, Inan MF, Reinhardt F, Weinberg RA. The Outgrowth of Micrometastases Is Enabled by the Formation of Filopodium-like Protrusions. Cancer Discov. 2012 Aug;2(8):706–21.
80. Bragado P, Estrada Y, Parikh F, Krause S, Capobianco C, Farina HG, et al. TGF-β2 dictates disseminated tumour cell fate in target organs through TGF-β-RIII and p38α/β signalling. Nat Cell Biol. 2013 Oct 27;15(11):1351–61.
81. Kobayashi A, Okuda H, Xing F, Pandey PR, Watabe M, Hirota S, et al. Bone morphogenetic protein 7 in dormancy and metastasis of prostate cancer stem-like cells in bone. J Exp Med. 2011 Dec 19;208(13):2641–55.
82. Sosa MS, Avivar-Valderas A, Bragado P, Wen H-C, Aguirre-Ghiso JA. ERK1/2 and p38α/β signaling in tumor cell quiescence: opportunities to control dormant residual disease. Clin Cancer Res. 2011 Sep 15;17(18):5850–7.
83. Malanchi I, Santamaria-Martínez A, Susanto E, Peng H, Lehr H-A, Delaloye J-F, et al. Interactions between cancer stem cells and their niche govern metastatic colonization. Nature. 2011 Dec 7;481(7379):85–9.

84. Mani SA, Guo W, Liao M-J, Eaton EN, Ayyanan A, Zhou AY, et al. The Epithelial-Mesenchymal Transition Generates Cells with Properties of Stem Cells. Cell. 2008 May 16;133(4):704–15.
85. Brabletz T. To differentiate or not — routes towards metastasis. Nat Rev Cancer. 2012 May 11;12(6):425–36.
86. Paget S. The distribution of secondary growths in cancer of the breast. Lancet. 1889 Mar;133(3421):571–3.
87. Langley RR, Fidler IJ. The seed and soil hypothesis revisited-The role of tumor-stroma interactions in metastasis to different organs. Int J Cancer. 2011 Jun 1;128(11):2527–35.
88. Lambert AW, Pattabiraman DR, Weinberg RA. Emerging Biological Principles of Metastasis. Cell. 2017;168(4):670–91.
89. Friedl P, Locker J, Sahai E, Segall JE. Classifying collective cancer cell invasion. Nat Cell Biol. 2012 Aug 1;14(8):777–83.
90. Einenkel J, Braumann U-D, Horn L-C, Kuska J-P, Höckel M. 3-D analysis of the invasion front in squamous cell carcinoma of the uterine cervix: histopathologic evidence for collective invasion per continuitatem. Anal Quant Cytol Histol. 2007 Oct;29(5):279–90.
91. Kadota K, Nitadori J, Woo KM, Sima CS, Finley DJ, Rusch VW, et al. Comprehensive Pathological Analyses in Lung Squamous Cell Carcinoma: Single Cell Invasion, Nuclear Diameter, and Tumor Budding Are Independent Prognostic Factors for Worse Outcomes. J Thorac Oncol. 2014 Aug;9(8):1126–39.
92. Lamouille S, Xu J, Derynck R. Molecular mechanisms of epithelial-mesenchymal transition. Nat Rev Mol Cell Biol. 2014 Mar;15(3):178–96.
93. Miettinen PJ, Ebner R, Lopez AR, Derynck R. TGF-beta induced transdifferentiation of mammary epithelial cells to mesenchymal cells: involvement of type I receptors. J Cell Biol. 1994 Dec;127(6 Pt 2):2021–36.
94. Maître J-L, Heisenberg C-P. Three Functions of Cadherins in Cell Adhesion. Curr Biol. 2013 Jul;23(14):R626–33.
95. Gravdal K, Halvorsen OJ, Haukaas SA, Akslen LA. A Switch from E-Cadherin to N-Cadherin Expression Indicates Epithelial to Mesenchymal Transition and Is of Strong and Independent Importance for the Progress of Prostate Cancer. Clin Cancer Res. 2007 Dec 1;13(23):7003–11.
96. Asnaghi L, Vass WC, Quadri R, Day PM, Qian X, Braverman R, et al. E-cadherin

negatively regulates neoplastic growth in non-small cell lung cancer: role of Rho GTPases. Oncogene. 2010 May 13;29(19):2760–71.

97. Al-Saad S, Al-Shibli K, Donnem T, Persson M, Bremnes RM, Busund L-T. The prognostic impact of NF-κB p105, vimentin, E-cadherin and Par6 expression in epithelial and stromal compartment in non-small-cell lung cancer. Br J Cancer. 2008 Nov 4;99(9):1476–83.
98. Satelli A, Li S. Vimentin in cancer and its potential as a molecular target for cancer therapy. Cell Mol Life Sci. 2011 Sep;68(18):3033–46.
99. Broers JL, de Leij L, Rot MK, ter Haar A, Lane EB, Leigh IM, et al. Expression of intermediate filament proteins in fetal and adult human lung tissues. Differentiation. 1989 May;40(2):119–28.
100. Upton MP, Hirohashi S, Tome Y, Miyazawa N, Suemasu K, Shimosato Y. Expression of vimentin in surgically resected adenocarcinomas and large cell carcinomas of lung. Am J Surg Pathol. 1986 Aug;10(8):560–7.
101. Luo J, Zuo J, Wu J, Wan P, Kang D, Xiang C, et al. In vivo RNAi screen identifies candidate signaling genes required for collective cell migration in Drosophila ovary. Sci China Life Sci. 2015 Apr 20;58(4):379–89.
102. Seals DF, Azucena EF, Pass I, Tesfay L, Gordon R, Woodrow M, et al. The adaptor protein Tks5/Fish is required for podosome formation and function, and for the protease-driven invasion of cancer cells. Cancer Cell. 2005 Feb;7(2):155–65.
103. Blouw B, Patel M, Iizuka S, Abdullah C, You WK, Huang X, et al. The Invadopodia Scaffold Protein Tks5 Is Required for the Growth of Human Breast Cancer Cells In Vitro and In Vivo. Tan M, editor. PLoS One. 2015 Mar 31;10(3):e0121003.
104. Jacob A, Linklater E, Bayless BA, Lyons T, Prekeris R. The role and regulation of Rab40b-Tks5 complex during invadopodia formation and cancer cell invasion. J Cell Sci. 2016 Dec 1;129(23):4341–53.
105. Paterson EK, Courtneidge SA. Invadosomes are coming: new insights into function and disease relevance. FEBS J. 2017 Jun 22;
106. Jayo A, Parsons M. Fascin: A key regulator of cytoskeletal dynamics. Int J Biochem Cell Biol. 2010 Oct;42(10):1614–7.
107. Zhang F-R, Tao L-H, Shen Z-Y, Lv Z, Xu L-Y, Li E-M. Fascin Expression in Human Embryonic, Fetal, and Normal Adult Tissue. J Histochem Cytochem. 2008 Feb 15;56(2):193–9.
108. Ma Y, Machesky LM. Fascin1 in carcinomas: Its regulation and prognostic value. Int

J Cancer. 2015 Dec 1;137(11):2534–44.

109. Li A, Dawson JC, Forero-Vargas M, Spence HJ, Yu X, König I, et al. The actin-bundling protein fascin stabilizes actin in invadopodia and potentiates protrusive invasion. Curr Biol. 2010 Feb 23;20(4):339–45.
110. Roskoski R. ERK1/2 MAP kinases: Structure, function, and regulation. Pharmacol Res. 2012 Aug;66(2):105–43.
111. Vicent S, López-Picazo JM, Toledo G, Lozano MD, Torre W, Garcia-Corchón C, et al. ERK1/2 is activated in non-small-cell lung cancer and associated with advanced tumours. Br J Cancer. 2004 Mar 8;90(5):1047–52.
112. Lawson ND, Mugford JW, Diamond BA, Weinstein BM. phospholipase C gamma-1 is required downstream of vascular endothelial growth factor during arterial development. Genes Dev. 2003 Jun 1;17(11):1346–51.
113. Jones NP, Peak J, Brader S, Eccles SA, Katan M. PLC 1 is essential for early events in integrin signalling required for cell motility. J Cell Sci. 2005 Jun 15;118(12):2695–706.
114. Phillips-Mason PJ, Kaur H, Burden-Gulley SM, Craig SEL, Brady-Kalnay SM. Identification of phospholipase C gamma1 as a protein tyrosine phosphatase mu substrate that regulates cell migration. J Cell Biochem. 2011 Jan;112(1):39–48.
115. Ridley AJ. Rho GTPase signalling in cell migration. Curr Opin Cell Biol. 2015 Oct;36:103–12.
116. Konstantinidou G, Ramadori G, Torti F, Kangasniemi K, Ramirez RE, Cai Y, et al. RHOA-FAK Is a Required Signaling Axis for the Maintenance of KRAS-Driven Lung Adenocarcinomas. Cancer Discov. 2013 Apr;3(4):444–57.
117. Stengel KR, Zheng Y. Essential Role of Cdc42 in Ras-Induced Transformation Revealed by Gene Targeting. Jackson M, editor. PLoS One. 2012 Jun 18;7(6):e37317.
118. Jiang JX, Penuela S. Connexin and pannexin channels in cancer. BMC Cell Biol. 2016 May 24;17 Suppl 1(Suppl 1):12.
119. Elzarrad MK, Haroon A, Willecke K, Dobrowolski R, Gillespie MN, Al-Mehdi A-B. Connexin-43 upregulation in micrometastases and tumor vasculature and its role in tumor cell attachment to pulmonary endothelium. BMC Med. 2008 Dec 22;6(1):20.
120. Wang Z-S, Wu L-Q, Yi X, Geng C, Li Y-J, Yao R-Y. Connexin-43 can delay early recurrence and metastasis in patients with hepatitis B-related hepatocellular carcinoma and low serum alpha-fetoprotein after radical hepatectomy. BMC Cancer. 2013 Jun 24;13:306.

121. Murphy PM, Baggiolini M, Charo IF, Hébert CA, Horuk R, Matsushima K, et al. International union of pharmacology. XXII. Nomenclature for chemokine receptors. Pharmacol Rev. 2000 Mar;52(1):145–76.
122. Raman D, Sobolik-Delmaire T, Richmond A. Chemokines in health and disease. Exp Cell Res. 2011 Mar 10;317(5):575–89.
123. Sarvaiya PJ, Guo D, Ulasov I, Gabikian P, Lesniak MS. Chemokines in tumor progression and metastasis. Oncotarget. 2013 Dec;4(12):2171–85.
124. Fernando RI, Castillo MD, Litzinger M, Hamilton DH, Palena C. IL-8 Signaling Plays a Critical Role in the Epithelial-Mesenchymal Transition of Human Carcinoma Cells. Cancer Res. 2011 Aug 1;71(15):5296–306.
125. Saintigny P, Massarelli E, Lin S, Ahn Y-H, Chen Y, Goswami S, et al. CXCR2 expression in tumor cells is a poor prognostic factor and promotes invasion and metastasis in lung adenocarcinoma. Cancer Res. 2013 Jan 15;73(2):571–82.
126. Jamieson T, Clarke M, Steele CW, Samuel MS, Neumann J, Jung A, et al. Inhibition of CXCR2 profoundly suppresses inflammation-driven and spontaneous tumorigenesis. J Clin Invest. 2012 Sep 4;122(9):3127–44.
127. Chatterjee S, Behnam Azad B, Nimmagadda S. The intricate role of CXCR4 in cancer. Adv Cancer Res. 2014;124:31–82.
128. Liu K, Bao C, Yao N, Miao C, Varlotto J, Sun Q, et al. Expression of CXCR4 and non-small cell lung cancer prognosis: a meta-analysis. Int J Clin Exp Med. 2015;8(5):7435–45.
129. Wang L, Wang Z, Liu X, Liu F. High-level C-X-C chemokine receptor type 4 expression correlates with brain-specific metastasis following complete resection of non-small cell lung cancer. Oncol Lett. 2014 Jun;7(6):1871–6.
130. Wang X, Haswell JR, Roberts CWM. Molecular Pathways: SWI/SNF (BAF) Complexes Are Frequently Mutated in Cancer--Mechanisms and Potential Therapeutic Insights. Clin Cancer Res. 2014 Jan 1;20(1):21–7.
131. Orvis T, Hepperla A, Walter V, Song S, Simon J, Parker J, et al. BRG1/SMARCA4 inactivation promotes non-small cell lung cancer aggressivenessby altering chromatin organization. Cancer Res. 2014;74(22):6486.
132. Herpel E, Rieker RJ, Dienemann H, Muley T, Meister M, Hartmann A, et al. SMARCA4 and SMARCA2 deficiency in non–small cell lung cancer: immunohistochemical survey of 316 consecutive specimens. Ann Diagn Pathol. 2017 Feb;26:47–51.

133. Bell EH, Chakraborty AR, Mo X, Liu Z, Shilo K, Kirste S, et al. SMARCA4/BRG1 Is a Novel Prognostic Biomarker Predictive of Cisplatin-Based Chemotherapy Outcomes in Resected Non-Small Cell Lung Cancer. Clin Cancer Res. 2016 May 15;22(10):2396–404.
134. Battifora H. The multitumor (sausage) tissue block: novel method for immunohistochemical antibody testing. Lab Invest. 1986 Aug;55(2):244–8.
135. Kononen J, Bubendorf L, Kallioniemi A, Bärlund M, Schraml P, Leighton S, et al. Tissue microarrays for high-throughput molecular profiling of tumor specimens. Nat Med. 1998 Jul;4(7):844–7.
136. Kampf C, Olsson I, Ryberg U, Sjöstedt E, Pontén F. Production of tissue microarrays, immunohistochemistry staining and digitalization within the human protein atlas. J Vis Exp. 2012 May 31;(63).
137. Pirozzi G, Tirino V, Camerlingo R, Franco R, La Rocca A, Liguori E, et al. Epithelial to Mesenchymal Transition by TGFβ-1 Induction Increases Stemness Characteristics in Primary Non Small Cell Lung Cancer Cell Line. Deb S, editor. PLoS One. 2011 Jun 30;6(6):e21548.
138. Yang M-H, Wu M-Z, Chiou S-H, Chen P-M, Chang S-Y, Liu C-J, et al. Direct regulation of TWIST by HIF-1α promotes metastasis. Nat Cell Biol. 2008 Mar 24;10(3):295–305.
139. Popper HH. Progression and metastasis of lung cancer. Cancer Metastasis Rev. 2016 Mar;35(1):75–91.
140. Smit MA, Geiger TR, Song J-Y, Gitelman I, Peeper DS. A Twist-Snail Axis Critical for TrkB-Induced Epithelial-Mesenchymal Transition-Like Transformation, Anoikis Resistance, and Metastasis. Mol Cell Biol. 2009 Jul 1;29(13):3722–37.
141. Jolly MK, Tripathi SC, Jia D, Mooney SM, Celiktas M, Hanash SM, et al. Stability of the hybrid epithelial/mesenchymal phenotype. Oncotarget. 2016 May 10;7(19):27067–84.
142. Mayor R, Etienne-Manneville S. The front and rear of collective cell migration. Nat Rev Mol Cell Biol. 2016 Jan 4;17(2):97–109.
143. Labernadie A, Kato T, Brugués A, Serra-Picamal X, Derzsi S, Arwert E, et al. A mechanically active heterotypic E-cadherin/N-cadherin adhesion enables fibroblasts to drive cancer cell invasion. Nat Cell Biol. 2017 Feb 20;19(3):224–37.
144. Zheng X, Carstens JL, Kim J, Scheible M, Kaye J, Sugimoto H, et al. Epithelial-to-mesenchymal transition is dispensable for metastasis but induces chemoresistance in

pancreatic cancer. Nature. 2015 Nov 11;527(7579):525–30.

145. Fischer KR, Durrans A, Lee S, Sheng J, Li F, Wong STC, et al. Epithelial-to-mesenchymal transition is not required for lung metastasis but contributes to chemoresistance. Nature. 2015 Nov 11;527(7579):472–6.
146. Tamura T, Kurishima K, Nakazawa K, Kagohashi K, Ishikawa H, Satoh H, et al. Specific organ metastases and survival in metastatic non-small-cell lung cancer. Mol Clin Oncol. 2015 Jan;3(1):217–21.
147. Fielding AB, Dobreva I, McDonald PC, Foster LJ, Dedhar S. Integrin-linked kinase localizes to the centrosome and regulates mitotic spindle organization. J Cell Biol. 2008 Feb 25;180(4):681–9.
148. Aceto N, Bardia A, Miyamoto DT, Donaldson MC, Wittner BS, Spencer JA, et al. Circulating Tumor Cell Clusters Are Oligoclonal Precursors of Breast Cancer Metastasis. Cell. 2014 Aug 28;158(5):1110–22.
149. Cheung KJ, Ewald AJ. A collective route to metastasis: Seeding by tumor cell clusters. Science (80-). 2016;352(6282).

APPENDIX

Table 4: Percentages of positive cases in total, as well as separately in AC, SCC, and LC

	All cases *(n=528)*	**AC** *(n=325)*	**SCC** *(n=142)*	**LC** *(n=61)*
E-cad	98.1%	98.8%	99.2%	91.7%
N-cad	99.6%	100%	100%	96.7%
pERK	67.2%	68.1%	54.4%	91.7%
Twist	65.4%	50.7%	83.8%	78.4%
Vim	32.8%	34.5%	15.2%	47.6%
Mad	81.5%	82.2%	81.0%	80.0%
Tks5	48.8%	42.1%	73.2%	36.1%
PLCγ	55.6%	53.1%	53.7%	65.0%
Con43	70.1%	59.4%	94.2%	73.8%

Table 5: Mean staining intensity (in score [0-2] for E-cad, N-cad, and pERK) or mean staining extent (in %) for Twist, Vim, Mad, Tks5, PLCγ, and Con43

	All cases *(n=528)*	**AC** *(n=325)*	**SCC** *(n=142)*	**LC** *(n=61)*
E-cad (0-2)	1.13	1.09	1.23	1.07
N-cad (0-2)	1.10	1.13	1.08	1.02
pERK (0-2)	0.71	0.73	0.47	1.03
Twist (%)	24.8%	17.2%	40.6%	29.7%
Vim (%)	8.9%	7.6%	7.2%	19.9%
Mad (%)	33.5%	34.9%	31.6%	31.2%
Tks5 (%)	7.8%	4.3%	16.5%	6.7%
PLCγ (%)	14.1%	14.8%	13.2%	12.2%
Con43 (%)	29.0%	18.3%	53.1%	30.4%

Table 6: Percentages of positive cases in the validation set in comparison to the study set

	Validation set (n=528)	**Study set - center** *(n=30)*	**Study set - invasion** *(n=30)*
E-cad	98.1%	100%	100%
N-cad	99.6%	100%	100%
pERK	67.2%	33.3%	53.3%
Twist	65.4%	100%	100%
Vim	32.8%	0%	30.0%
Mad	81.5%	76.7%	76.7%
Tks5	48.8%	0%	70.0%
PLCγ	55.6%	0%	73.3%
Con43	70.1%	66.7%	66.7%